GL-TR-90-0351

Scintillation and In-situ Irregularity Parameters in the Auroral Oval and Polar Cap

Eileen MacKenzie
Sunanda Basu
Paul Pruneau

Boston College
Institute for Space Research
Newton MA 02159

28 December 1990

Scientific Report No. 1

Approved for public release; distribution unlimited

GEOPHYSICS LABORATORY
AIR FORCE SYSTEMS COMMAND
UNITED STATES AIR FORCE
HANSCOM AIR FORCE BASE, MASSACHUSETTS 01731-5000

"This technical report has been reviewed and is approved for publication"

JAMES A. WHALEN
Contract Manager

JURGEN BUCHAU
Acting Branch Chief

FOR THE COMMANDER

ROBERT A. SKRIVANEK
Division Director

This report has been reviewed by the ESD Public Affairs Office (PA) and is releasable to the National Technical Information Service (NTIS).

Qualified requestors may obtain additional copies from the Defense Technical Information Center. all others should apply to the National Technical Information Service.

If your address has changed, or if you wish to be removed from the mailing list, or if the addressee is no longer employed by your organization, please notify GL/IMA, Hanscom AFB, MA 01731. This will assist us in maintaining a current mailing list.

Do not return copies of this report unless contractual obligations or notices on a specific document requires that it be returned.

UNCLASSIFIED

SECURITY CLASSIFICATION OF THIS PAGE

REPORT DOCUMENTATION PAGE

1a. REPORT SECURITY CLASSIFICATION: UNCLASSIFIED	1b. RESTRICTIVE MARKINGS: None
2a. SECURITY CLASSIFICATION AUTHORITY	3. DISTRIBUTION/AVAILABILITY OF REPORT: Approved for public release; distribution unlimited.
2b. DECLASSIFICATION/DOWNGRADING SCHEDULE	
4. PERFORMING ORGANIZATION REPORT NUMBER(S)	5. MONITORING ORGANIZATION REPORT NUMBER(S): GL-TR-90-0351
6a. NAME OF PERFORMING ORGANIZATION: Boston College Institute for Space Research; 6b. OFFICE SYMBOL (If applicable)	7a. NAME OF MONITORING ORGANIZATION: Geophysics Laboratory
6c. ADDRESS (City, State and ZIP Code): Newton MA 02159	7b. ADDRESS (City, State and ZIP Code): Hanscom AFB MA 01731-5000
8a. NAME OF FUNDING/SPONSORING ORGANIZATION; 8b. OFFICE SYMBOL (If applicable)	9. PROCUREMENT INSTRUMENT IDENTIFICATION NUMBER: F19628-90-K-0007
8c. ADDRESS (City, State and ZIP Code)	10. SOURCE OF FUNDING NOS.

PROGRAM ELEMENT NO.	PROJECT NO.	TASK NO.	WORK UNIT NO.
61102F	2310	G9	AM

11. TITLE (Include Security Classification): Scintillation & In-Situ Irregularity Parameters in the Auroral Oval and Polar Cap

12. PERSONAL AUTHOR(S): Eileen MacKenzie, Sunanda Basu, Paul Pruneau

13a. TYPE OF REPORT	13b. TIME COVERED	14. DATE OF REPORT (Yr., Mo., Day)	15. PAGE COUNT
Scientific #1	FROM 28Nov89 TO 28Nov90	1990 December 28	36

16. SUPPLEMENTARY NOTATION

17. COSATI CODES			18. SUBJECT TERMS (Continue on reverse if necessary and identify by block number)	
FIELD	GROUP	SUB. GR.	Amplitude & Phase Scintillation	Auroral Oval
			In-situ Density	Polar Cap
			Electron Density Deviation	Sunspot Cycle Variation

19. ABSTRACT (Continue on reverse if necessary and identify by block number)

The orbiting HiLat satellite launched by the Defense Nuclear Agency in 1983 offered a unique opportunity for studying ionospheric scintillation parameters in relation to in-situ irregularity parameters. An earlier report (AFGL-TR-87-0245) summarized our findings during the sunspot minimum period of 1983-1985 for data obtained at Tromso, Norway. In this report, we extend our study to the sunspot maximum period of 1988-1989. For completeness, we augment the HiLat scintillation data by phase and amplitude scintillation morphology obtained with the help of the quasi-geostationary polar beacon satellites at Tromso during the period 1988 to 1990. To contrast these two distinct high latitude regions, we provide scintillation morphology using polar beacon satellites from Thule, Greenland for the period 1987 to 1990. Some new findings emerge on the UT and seasonal variation of high latitude scintillation as a result of this study.

20. DISTRIBUTION/AVAILABILITY OF ABSTRACT	21. ABSTRACT SECURITY CLASSIFICATION	
UNCLASSIFIED/UNLIMITED ☒ SAME AS RPT. ☐ OTIC USERS ☐	UNCLASSIFIED	
22a. NAME OF RESPONSIBLE INDIVIDUAL: James Whalen	22b. TELEPHONE NUMBER (Include Area Code): (617) 377-4766	22c. OFFICE SYMBOL: GL/LIS

DD FORM 1473, 83 APR EDITION OF 1 JAN 73 IS OBSOLETE.

UNCLASSIFIED

SECURITY CLASSIFICATION OF THIS PAGE

ACKNOWLEDGEMENTS

The authors thank Santimay Basu of the Ionospheric Physics Division, Phillips Laboratory, who made the report possible by making the scintillation data available and for providing helpful advice. We also thank F.J. Rich of the Space Physics Division, Phillips Laboratory, for providing the ion density data from HiLat. We appreciate the efforts of R.C. Livingston of SRI International for his help with the radio beacon data analysis, and Elizabeth Galligan of Boston College for assistance with the polar beacon satellite data analysis.

The work was supported by GL Contract F19628-90-K-0007 with Boston College.

1. INTRODUCTION

The morphological features of scintillation regions have been examined in a wide variety of studies (cf. reviews by Aarons, 1982; Basu et al., 1988 and references therein). However, even such a plethora of earlier publications has failed to clearly delineate the different variables on which scintillation depends, particularly at high latitudes. This is because recent studies have shown that in the polar and auroral environment, large-scale ionization transport in the form of "patches" has an important role to play in determining scintillation behavior (Buchau et al., 1985; Weber et al., 1984; 1986; Basu et al., 1989; 1990). Thus, Tsunoda (1988), in his comprehensive review, points out that attention has been diverted from "local" type of mechanisms, such as particle precipitation, to processes such as global electrodynamics and convective control of patch formation by the interplanetary magnetic field (IMF).

It is the intent of this report to extend the measurements of scintillations and in-situ parameters presented in an earlier study using HiLat (MacKenzie et al., 1987, to be referred to as Report I) by more recent measurements using the same satellite during the current sunspot maximum. We also augment these measurements with those of long-term scintillations from polar beacon satellites at Tromso and Thule which allow us to better study the effects of transport.

2. THE HiLat DATA BASE

As detailed in Report I, the HiLat satellite was designed to provide quantitative information on high latitude scintillation through radio beacon experiments, accompanied by in-situ data to define the background ionospheric processes (Fremouw et al., 1985). We concentrate on the HiLat satellite observations performed by the Air Force Geophysics Laboratory at Tromso, Norway (66° Λ). Under quiet magnetic conditions, this station is within the nightside auroral oval while the dayside oval is poleward of the station. This report will focus on observations made in 1988-89, a period of increasing solar sunspot number. Figure 1 illustrates the drastic variation of both the monthly mean and smoothed sunspot numbers from December 1983 to March 1990. During the time frame of the observations shown in Report I, namely 1984-85, smoothed sunspot number declined from approximately 60 to 15. Within the time frame of observations to be examined in this report, namely 1988-89, smoothed sunspot number increased from approximately 60 to 160.

The phase and amplitude scintillation magnitudes are examined in the spatial and temporal frames of invariant latitude (Λ) and magnetic local time (MLT). As in the previous analysis, scintillation measurements have been made on a sliding 30-sec window with values computed every 15 sec at the midpoint of the window for the length of each pass. These have then been merged into seasonal data bases, deleting data acquired below a satellite elevation angle of 20°. The parameters to be discussed in this report are the 137-MHz phase and intensity scintillation observations and the in-situ ion density at the satellite altitude. For definitions of phase and amplitude scintillation indices, the reader is referred to Report I. The phase and intensity scintillations are assumed to pertain to the 350 km sub-ionospheric intersection point of the satellite as observed from Tromso, while the in-situ parameters are measured at the height of the satellite (830 km). Each 15-sec scintillation value, both phase and intensity, has been corrected for ionospheric zenith angle (i) by means of a $(\sec i)^{1/2}$ correction. Median values of the corrected rms phase deviation, σ_ϕ, and intensity scintillation, S_4, and the ion density have been calculated in 2.5°Λ - 1-hr MLT bins for each season. Bins with fewer than 10 points have been

omitted. These seasonal data bases have been further sorted into two groups: those observed under magnetically quiet conditions (Kp < 3.5) and those under magnetically disturbed conditions (Kp > 3.5). Results of such statistical analyses are given below.

2.1. RMS Phase Deviation

Figures 2a - 2c illustrate, in polar plots of invariant latitude-MLT, the median rms phase deviation, σ_ϕ, of 137 MHz scintillation for 3 equinoxes: Feb-Apr 1984, Feb-Apr 1988, and Feb-Apr 1989. The 1984 season is included to facilitate comparison with data in the earlier report. The 1984 and 1988 seasons have similar features and scintillation levels: low σ_ϕ values are present on the dayside while maximum σ_ϕ is seen in the region of L-shell enhancement on the nightside. The Feb-Apr 1989 data shows a similar pattern but with much higher σ_ϕ in each bin. A common scale for all panels results in a deceptive broadening of the L-shell enhancement region. Figure 3 presents the rms phase deviation, σ_ϕ, in a different format. This figure utilizes a midnight-noon cut through the dial plots of Figures 2b and 2c to obtain in a more quantitative manner the variation of σ_ϕ with invariant latitude in the 2-hr MLT time period centered on midnight and noon. We have broadened this data set to include all seasons between Feb-Apr 1988 and Feb-Apr 1989. In these cuts, both the gradual increase of rms phase deviation, σ_ϕ, with each season and the pronounced enhancement on the nightside over the latitude range 65° - 67.5°Λ can be seen. This enhancement, occurring where the satellite ray path achieves alignment with the magnetic L-shell oriented irregularities, was the most stable morphological feature in Report I. This has also been noted by MacDougall (1990).

2.2. Intensity Scintillation, S_4

Figures 4a - 4c illustrate, in polar plots of invariant latitude-MLT, the median 137 MHz intensity scintillation magnitudes, S_4, for 3 equinoxes: Feb-Apr 1984, Feb-Apr 1988, and Feb-Apr 1989. The 1984 and 1988 seasons are similar in features and scintillation level, while the 1989 data show increased intensity scintillation magnitudes particularly in the midnight and noontime sectors. The nighttime enhancement of intensity scintillation index, S_4, in the region

of alignment of the ray path with the magnetic L-shell is less pronounced than was seen for the phase scintillation. The L-shell alignment of the km-scale irregularities causing intensity scintillation appears weaker than the tens of kilometers scale that controls the phase scintillations. In Figure 5, the intensity scintillation, S_4, is presented in the format of a midnight-noon cut through the dial plots of Figures 4b and 4c. Additional seasons have been included. In these cuts, the intensity scintillation, S_4, is seen to increase with each season.

2.3. Ion Density

The in-situ ion density has been observed to vary with both solar activity and season. Report I has shown the invariant latitude-MLT variation of this parameter during 1984-85, a low sunspot period. The median ion density showed a seasonal maximum in Feb-Jul with a daytime diurnal maximum. Figures 6a - 6c illustrate the invariant latitude-MLT ion density variation during Feb-Apr 1984, Feb-Apr 1988, and Feb-Apr 1989. The 1984 and 1988 data are comparable while the Feb-Apr 1989 data show an enormous increase; the minimum ion density in 1989 is an order of magnitude greater than those of 1984 or 1988. Figure 6c has been redone on a different scale in Figure 6d to exhibit some of the variation lost when the scale, appropriate for 1984 and 1988, is used for 1989. Figure 7 illustrates the midnight-noon cuts through the polar plots of Figures 6b and 6d. Additional seasons between Feb-Apr 1988 and Feb-Apr 1989 are included. Although sunspot number was increasing throughout 1988, the large increase in ion density does not show in the statistics until Feb-Apr 1989, probably because the seasonal variations noted in Report I get masked by the ramp-like increase in smoothed sunspot number.

3. SCINTILLATION MEASUREMENTS FROM QUASI-GEOSTATIONARY SATELLITES

Additional quasi-geostationary scintillation data bases are available to augment the HiLat orbiting satellite statistics. The major difference between HiLat scintillation data and those obtained from quasi-geostationary satellites is that in the latter, irregularity anisotropy does not play a major role so that long-term trends are more readily discernible. Measurements using several polar beacon satellites at 250 MHz are available for similar time periods. Auroral oval data are obtained in the Scandinavian sector from Tromso, while polar cap data are available from Thule. These polar beacon satellites do not provide uniform local time coverage. They also tend to explore different latitude ranges at different times of the year. Results from each station are given below.

3.1. Measurements at Tromso

At Tromso, the polar beacons provide 24-hour coverage in a combination of data from within the auroral oval with that from slightly below it. Basu et al. (1988) have shown very low intensity scintillation statistics during the sunspot minimum period of 1984-86, with fades of 5 dB approximately 5% of the time. From the current sunspot maximum 250 MHz data, both intensity and phase scintillation data are utilized. This has been subdivided to focus on only auroral location data for nighttime hours of 21-03 MLT. Figure 8 illustrates the median S_4 and rms phase deviation, σ_ϕ, statistics seasonally from November 1985 to January 1990. The S_4 median shows low values through the sunspot minimum years (1985-1987) increasing late in 1988. The σ_ϕ median exhibits less pronounced variation. However, both S_4 and σ_ϕ show a pronounced seasonal variation with minimum scintillation occurrence seen in the Summer months. A similar minimum was observed in the Goose Bay auroral scintillation data (Basu et al. 1988). We shall discuss this point further in Section 4.

3.2. Measurements at Thule

The polar cap data, available from Thule, likewise explores different latitude ranges between 85° - 88° invariant at different times of the year. However, this range is within the

central polar cap so that no subdivision of the data has been performed. Figures 9a and 9b illustrate the percent occurrence of varying intensity scintillation fade levels over a whole solar cycle, 1979-1990, while Figure 10 illustrates the median S_4 and rms phase deviation, σ_ϕ, statistics seasonally over a shorter time frame (1987-1989). As was seen with the Tromso data, a larger variation with increased sunspot number is seen in S_4 than in σ_ϕ. Both Figures 9 and 10 show a minimum in scintillation occurrence and magnitude during the local Summer months.

To study this behavior in greater detail, we present the scintillation fade occurrence > 4 dB during sunspot minimum (July 1985 - June 1986) and sunspot maximum (July 1989 - June 1990) periods in Figures 11 and 12. It should be noted that a fade of 4 dB is equivalent to peak-to-peak fluctuations of 6 dB (Whitney, 1974). Figure 12 clearly shows minimal scintillation occurrence during Summer, and a diffuse maximum between October to February. Largest percentage occurrence is observed between 15 - 06 UT. To study the occurrence of intense scintillation events, we show in Figure 13, contours of a fade level >10 dB (peak-to-peak fluctuations of 15 dB) during the high sunspot year of 1989-90. The same seasonal pattern is emphasized with the highest activity being confined to 18 - 24 UT. There is a general tendency for somewhat greater scintillation occurrence in the Fall as compared with the Spring, as Figures 9a and 9b also depict. It is noteworthy that the time of maximum occurrence is not related to total darkness, as the sunset and sunrise times at 110-km altitude indicate for the equinoxes. At the solstices, of course, there is either no sunrise in the winter months or no sunset in the summer months. Thus, the occurrence of scintillation at Thule does not seem to be controlled by local conditions. We shall discuss this point further in the next Section.

4. DISCUSSION

The major morphological finding of the HiLat scintillation study, namely, the enhancement of scintillation where the satellite ray path was aligned with the magnetic L-shell oriented irregularities, has been discussed at length in Report I. Longer term variations, such as seasonal dependence of scintillations, are harder to identify in HiLat data (Rino and Matthews, 1980) because of the great sensitivity of the magnitude of scintillations on the irregularity anisotropy. Sunspot cycle effects are clearly evident both on scintillations and on the in-situ ion density. In fact, particularly in the nighttime data, the increase of scintillations with the sunspot number can be thought of as being caused by a modulation in the background density as both the scintillation and ion density magnitude increase by the same factor. Of course, here we make the tacit assumption that the in-situ data measured at 830 km altitude mimics the density variation at the maximum of the F-layer because it is that density which controls the scintillations.

The additional geo-stationary scintillation data from Tromso and Thule presented in Section 3 provide much new information when considered in tandem with earlier published work from Thule (Aarons et al., 1981), Goose Bay (Basu et al., 1988), and Narssarsuaq (Basu, 1975; Basu and Aarons, 1980). If we start with the Thule data which refers to the central polar cap, then we find that the UT seasonal and solar cycle dependence of scintillations are generally consistent with transport of plasma from sub-cusp latitudes taken in conjunction with the shorting effect of a sunlit E-region in the summer on F-region irregularities. Some unexplained time shifts do occur, however. For instance, the highest scintillation occurrence is observed at Thule between 18-24 UT (cf. Figure 13), whereas Figure 4 of Buchau et al. (1985) shows the UT variation of maximum F-region density at a sub-cusp location (73° invariant at noon magnetic local time) to peak about three hours earlier. It is generally believed that sub-cusp plasma is convected across the polar cap and structures in the anti-sunward convection field giving rise to scintillations (Weber et al., 1984; Basu et al., 1990). On this basis, one expects maximum scintillation occurrence to follow maximum density behavior with a phase lag of

30 mins to an hour, depending on the velocity range of these patches varying between 300 and 700 ms^{-1}. However, a phase lag of three hours is difficult to understand and factors such as transit delays and other irregularity source mechanisms have to be investigated.

The seasonal behavior of the Tromso polar beacon scintillations is very similar to that observed at Thule during sunspot maximum, with the predominant variation being an annual one with minimum in the Summer. As mentioned earlier, Goose Bay polar beacon data had yielded similar results. Thus all three sets taken together seem to indicate that, on the average, transport and E-region shorting both are important considerations. Earlier annual scintillation morphology studies based on Narssarsuaq ATS-3 data, which explored the equatorward edge of the auroral oval, showed dramatically different occurrence statistics with a summer maximum and a winter minimum (Basu, 1975; Basu and Aarons, 1980). These earlier measurements were also at a frequency of 137 MHz so could respond to much weaker irregularities. However, this great difference in the occurrence characteristics between the poleward and equatorward regions of the auroral oval merit much further study. It is hoped that the routine polar beacon measurements from Sondrestrom started in 1990 will be helpful in providing further clues regarding this disagreement.

REFERENCES

Aarons, J. (1982) Global morphology of ionospheric scintillation, *Proc. IEEE, 70*: 360.

Aarons, J., J.P. Mullen, H.E. Whitney, A.L. Johnson, and E.J. Weber (1981) UHF scintillation activity over polar latitudes, *Geophys. Res. Lett., 8*: 277.

Basu, S., E. MacKenzie and Su. Basu (1988) Ionospheric constraints on VHF/UHF communications links during solar maximum and minimum periods, *Radio Sci., 23*: 363.

Basu, S., Su. Basu, C.E. Valladares, E.J. Weber, J. Buchau, G.J. Bishop, and B.W. Reinisch (1989) Coordinated observations of high latitude ionospheric turbulence, *SPI Conference Proceedings and Reprint Series, 8*: 137.

Basu, Su. (1975) Universal time seasonal variations of auroral zone magnetic activity and VHF scintillations, *J. Geophys. Res., 80*: 4725.

Basu, Su. and J. Aarons (1980) The morphology of high-latitude VHF scintillation near 70°W, *Radio Sci., 15*: 59.

Basu, Su., S. Basu, E.J. Weber, and G.J. Bishop (1990) Plasma structuring in the polar cap, *J. Geomag Geoelectr., 42*: 763.

Buchau, J., E.J. Weber, D.N. Anderson, H.C. Carlson, Jr., J.G. Moore, B.W. Reinisch, and R.C. Livingston (1985) Ionospheric structures in the polar cap: their origin and relation to 250-MHz scintillation, *Radio Sci., 20*: 325.

Fremouw, E.J., H.C. Carlson, T.A. Potemra, P.F. Bythrow, C.L. Rino, J.F. Vickrey, R.L. Livingston, R.E. Huffman, C.-I. Meng, D.A. Hardy, F.J. Rich, R.A. Heelis, W.B. Hanson, and L.A. Wittwer (1985) HiLat satellite mission, *Radio Sci., 20*: 416.

MacDougall, J. (1990) Distribution of irregularities in the northern polar region determined from HiLat observations, *Radio Sci., 25*: 115.

MacKenzie, E., S. Basu, and Su. Basu (1987) Ionospheric scintillations/TEC and in-situ density measurements at an auroral location in the European sector, AFGL-TR-87-0245, 14 August, ADA205543.

Rino, C.L. and S.J. Matthews (1980) On the morphology of auroral zone radio wave scintillation, *J. Geophys. Res., 85*: 4139.

Tsunoda, R.T. (1988) High-latitude F-region irregularities: a review and synthesis, *Rev. Geophys., 26*: 719.

Weber, E.J., J. Buchau, J.G. Moore, J.R. Sharber, R.C. Livingston, J.D. Winningham, and B.W. Reinisch (1984) F-layer ionization patches in the polar cap, *J. Geophys. Res., 89*: 1683.

Weber, E.J., J.A. Klobuchar, J. Buchau, H.C. Carlson, Jr., R.C. Livingston, O. de la Beaujardiere, M. McCready, J.G. Moore, and G.J. Bishop (1986), Polar cap F layer patches: structure and dynamics, *J. Geophys. Res., 91*: 12121.

Whitney, H.E. (1974) Notes on the relationship of scintillation index to probability distributions and their uses for system design, AFCRL-TR-74-0004, AD778092.

FIGURE CAPTIONS

Figure 1. Variation of monthly mean and smoothed sunspot numbers between December 1983 and March 1990.

Figure 2a. Variation of Tromso HiLat median rms phase deviation, σ_ϕ (137 MHz), with Invariant Latitude and magnetic local time under quiet magnetic conditions during Feb-Apr 1984.

Figure 2b. Variation of Tromso HiLat median rms phase deviation, σ_ϕ (137 MHz), with Invariant Latitude and magnetic local time under quiet magnetic conditions during Feb-Apr 1988.

Figure 2c. Variation of Tromso HiLat median rms phase deviation, σ_ϕ (137 MHz), with Invariant Latitude and magnetic local time under quiet magnetic conditions during Feb-Apr 1989.

Figure 3. Seasonal variations of 50th and 90th percentiles of Tromso HiLat rms phase deviation, σ_ϕ (137 MHz), with Invariant Latitude in 2-hr MLT bins along the midnight-noon meridian under quiet magnetic conditions in 1988-89.

Figure 4a. Variation of Tromso HiLat median S_4 (137 MHz), with Invariant Latitude and magnetic local time under quiet magnetic conditions during Feb-Apr 1984.

Figure 4b. Variation of Tromso HiLat median S_4 (137 MHz), with Invariant Latitude and magnetic local time under quiet magnetic conditions during Feb-Apr 1988.

Figure 4c. Variation of Tromso HiLat median S_4 (137 MHz), with Invariant Latitude and magnetic local time under quiet magnetic conditions during Feb-Apr 1989.

Figure 5. Seasonal variation of 50th and 90th percentiles of Tromso HiLat intensity scintillation, S_4 (137 MHz) with invariant latitude in 2-hr MLT bins along the midnight-noon meridian under quiet magnetic conditions in 1988-89.

Figure 6a. Variation of Tromso HiLat median ion density with Invariant Latitude and magnetic local time under quiet magnetic conditions during Feb-Apr 1984.

Figure 6b. Variation of Tromso HiLat median ion density with Invariant Latitude and magnetic local time under quiet magnetic conditions during Feb-Apr 1988.

Figure 6c. Variation of Tromso HiLat median ion density with Invariant Latitude and magnetic local time under quiet magnetic conditions during Feb-Apr 1989.

Figure 6d. Replotted version of Fig. 6c with a revised density scale in order to highlight increased ion density.

Figure 7. Seasonal variation of 50th and 90th percentiles of Tromso HiLat median ion density with invariant latitude in 2-hr MLT bins along the midnight-noon meridian under quiet magnetic conditions in 1988-89.

Figure 8. Seasonal variations of 50th and 90th percentiles of Tromso intensity scintillation, S_4 (250 MHz) and rms phase deviation, σ_φ (250 MHz) from quasi-geostationary satellites under quiet magnetic conditions within the auroral oval (~ 69°Λ) around magnetic local midnight (21-03 MLT) during 1985-1989.

Figure 9a. Occurrence of 5-, 10-, and 15- dB fades at 250 MHz observed using quasi-geostationary satellites at Thule during the period 1979-1986. All local times and all magnetic activity data are included.

Figure 9b. Occurrence of 5-, 10-, and 15- dB fades at 250 MHz observed using quasi-geostationary satellites at Thule during the period 1987-1990. All local times and all magnetic activity data are included.

Figure 10. Seasonal variations of 50th and 90th percentiles of Thule intensity scintillation, S_4 (250 MHz) and rms phase deviation, σ_φ (250 MHz) from quasi-geostationary satellites under all magnetic conditions around midnight (21-03 UT) during 1987-1989.

Figure 11. Contours of percent occurrence of fades > 4 dB at 250 MHz observed using quasi-geostationary satellites at Thule during the solar minimum period of July 1985 through June 1986 for all magnetic activity levels.

Figure 12. Contours of percent occurrence of fades > 4 dB at 250 MHz observed using quasi-geostationary satellites at Thule during the solar maximum period of July 1989 through June 1990 for all magnetic activity levels.

Figure 13. Contours of percent occurrence of fades > 10 dB at 250 MHz observed using quasi-geostationary satellites at Thule during the solar maximum period of July 1989 through June 1990 for all magnetic activity levels.

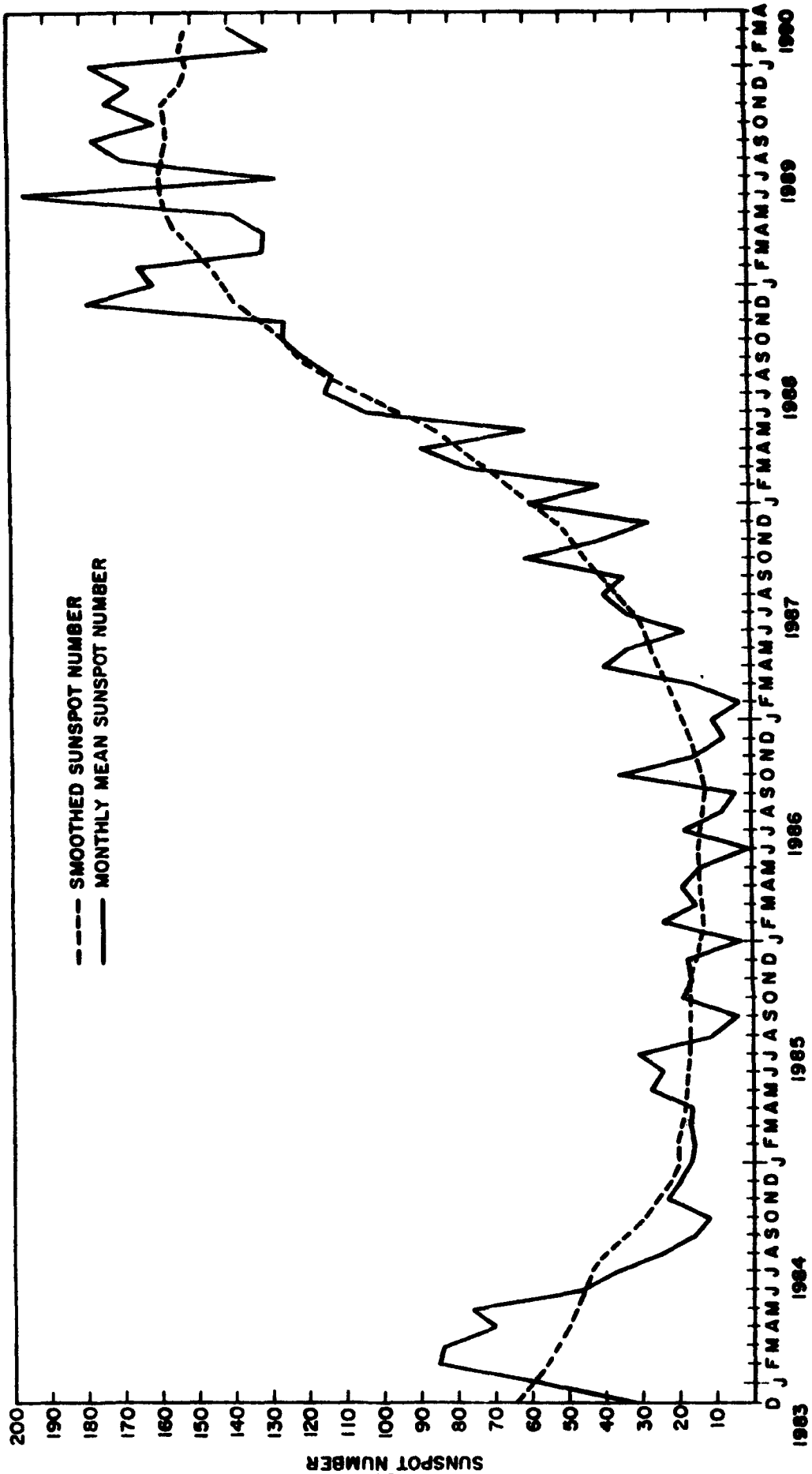
SMOOTHED SUNSPOT NUMBER
MONTHLY MEAN SUNSPOT NUMBER
SUNSPOT NUMBER
200
190
180
170
160
150
140
130
120
110
100
90
80
70
60
50
40
30
20
10
D J F M A M J J A S O N D J F M A M J J A S O N D J F M A M J J A S O N D J F M A M J J A S O N D J F M A M J J A S O N D J F M A
1983
1984
1985
1986
1987
1988
1989
1990

Figure 1.

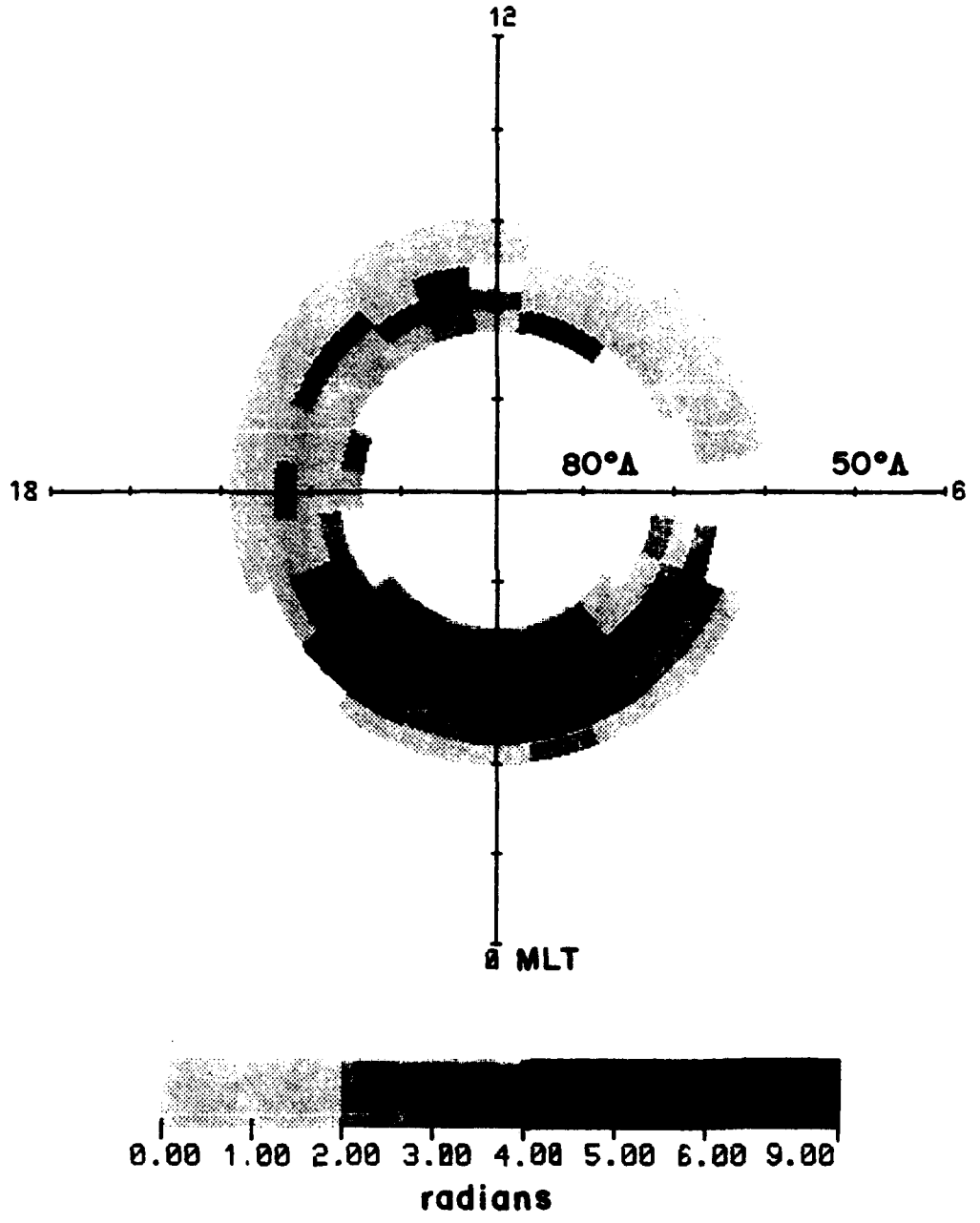
TROMSO HILAT 137 MHz
MEDIAN σ_ϕ (30 sec) Kp < 3.5
FEB-APR 84
12
18
6
80°Λ
50°Λ
0 MLT
0.00 1.00 2.00 3.00 4.00 5.00 6.00 9.00
radians

Figure 2a.

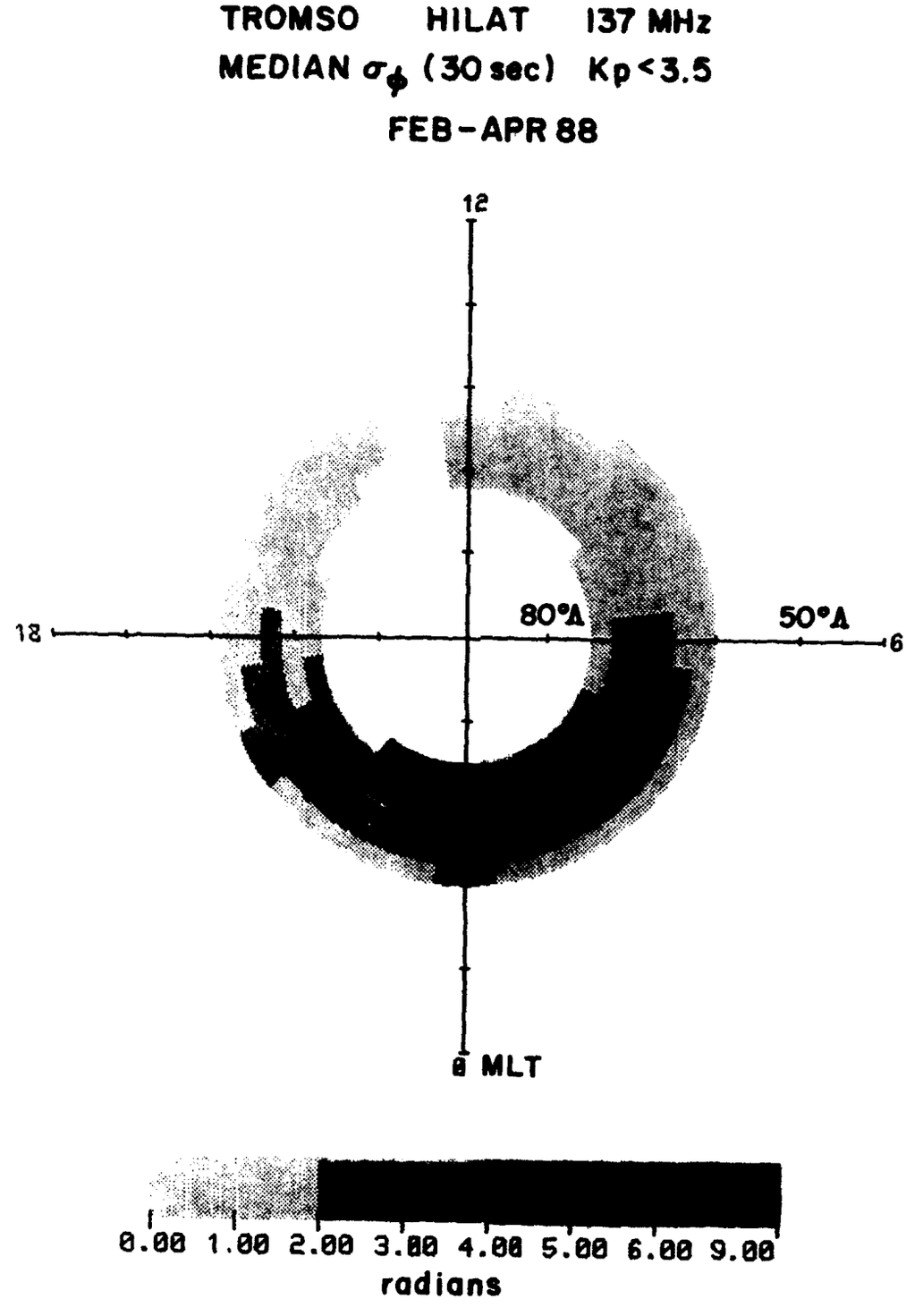
TROMSO HILAT 137 MHz
MEDIAN σ_ϕ (30 sec) Kp<3.5
FEB-APR 88
12
18
6
80°Λ
50°Λ
0 MLT
0.00 1.00 2.00 3.00 4.00 5.00 6.00 9.00
radians

Figure 2b.

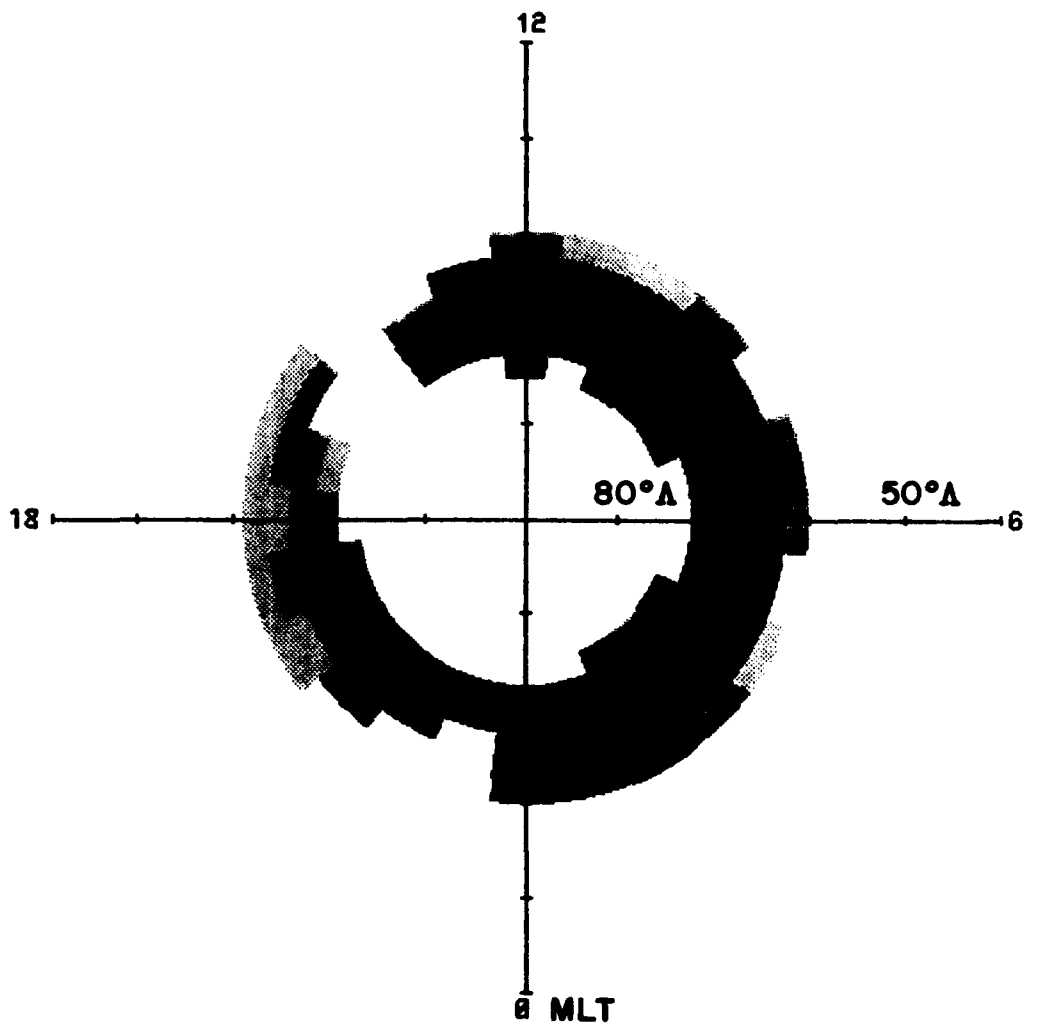
TROMSO HILAT 137 MHz
MEDIAN σ_ϕ (30 sec) Kp < 3.5
FEB-APR 89
12
18
6
80°Λ
50°Λ
0 MLT
0.00 1.00 2.00 3.00 4.00 5.00 6.00 9.00
radians

Figure 2c.

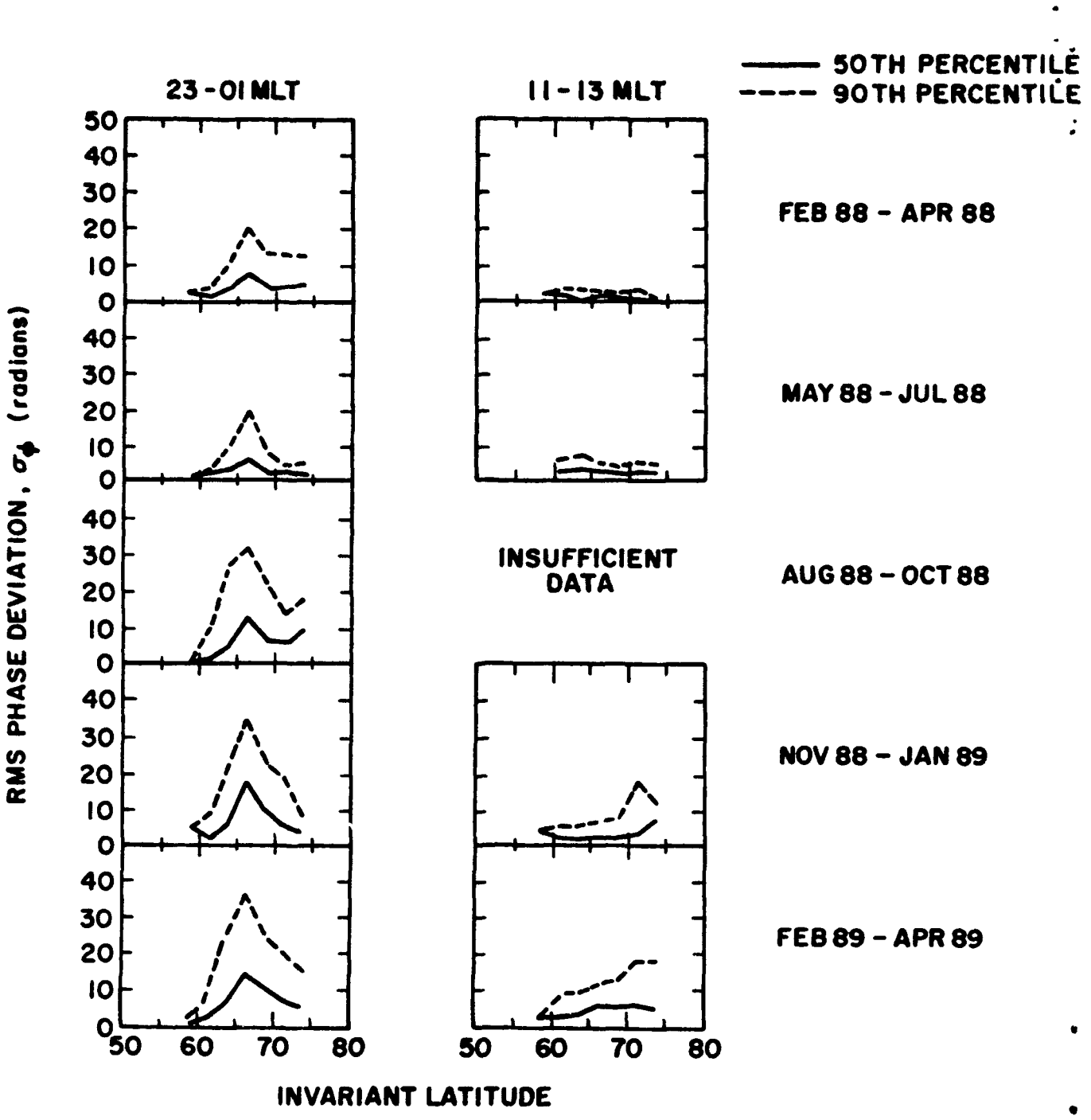
TROMSO HILAT σ_ϕ 137 MHz Kp < 3.5
50TH PERCENTILE
90TH PERCENTILE
23 - 01 MLT
11 - 13 MLT
FEB 88 - APR 88
MAY 88 - JUL 88
INSUFFICIENT DATA
AUG 88 - OCT 88
NOV 88 - JAN 89
FEB 89 - APR 89
RMS PHASE DEVIATION, σ_ϕ (radians)
INVARIANT LATITUDE
0
10
20
30
40
50
60
70
80

Figure 3.

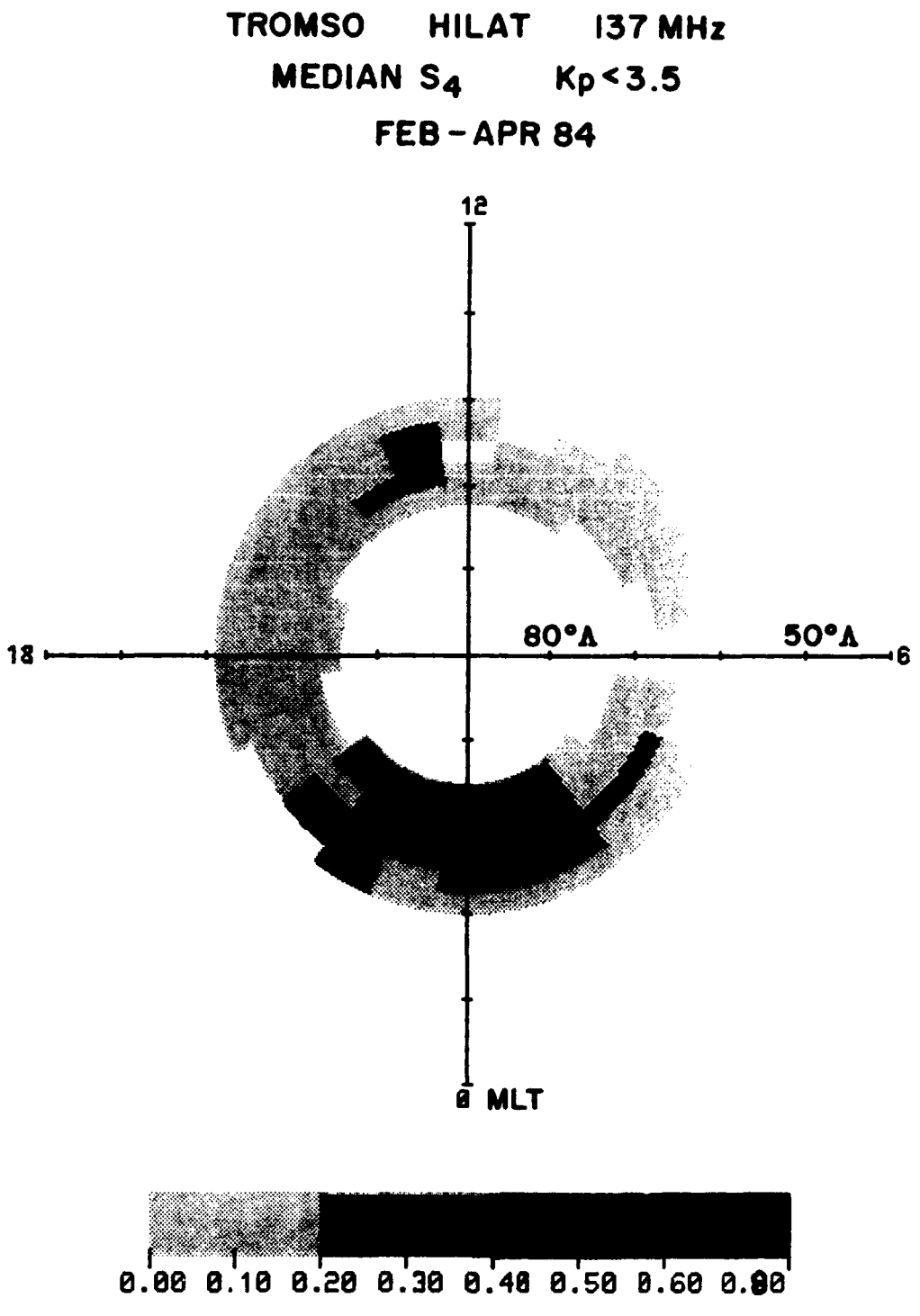
TROMSO HILAT 137 MHz
MEDIAN S_4 Kp<3.5
FEB-APR 84
12
18
6
80°Λ
50°Λ
0 MLT
0.00 0.10 0.20 0.30 0.40 0.50 0.60 0.80

Figure 4a.

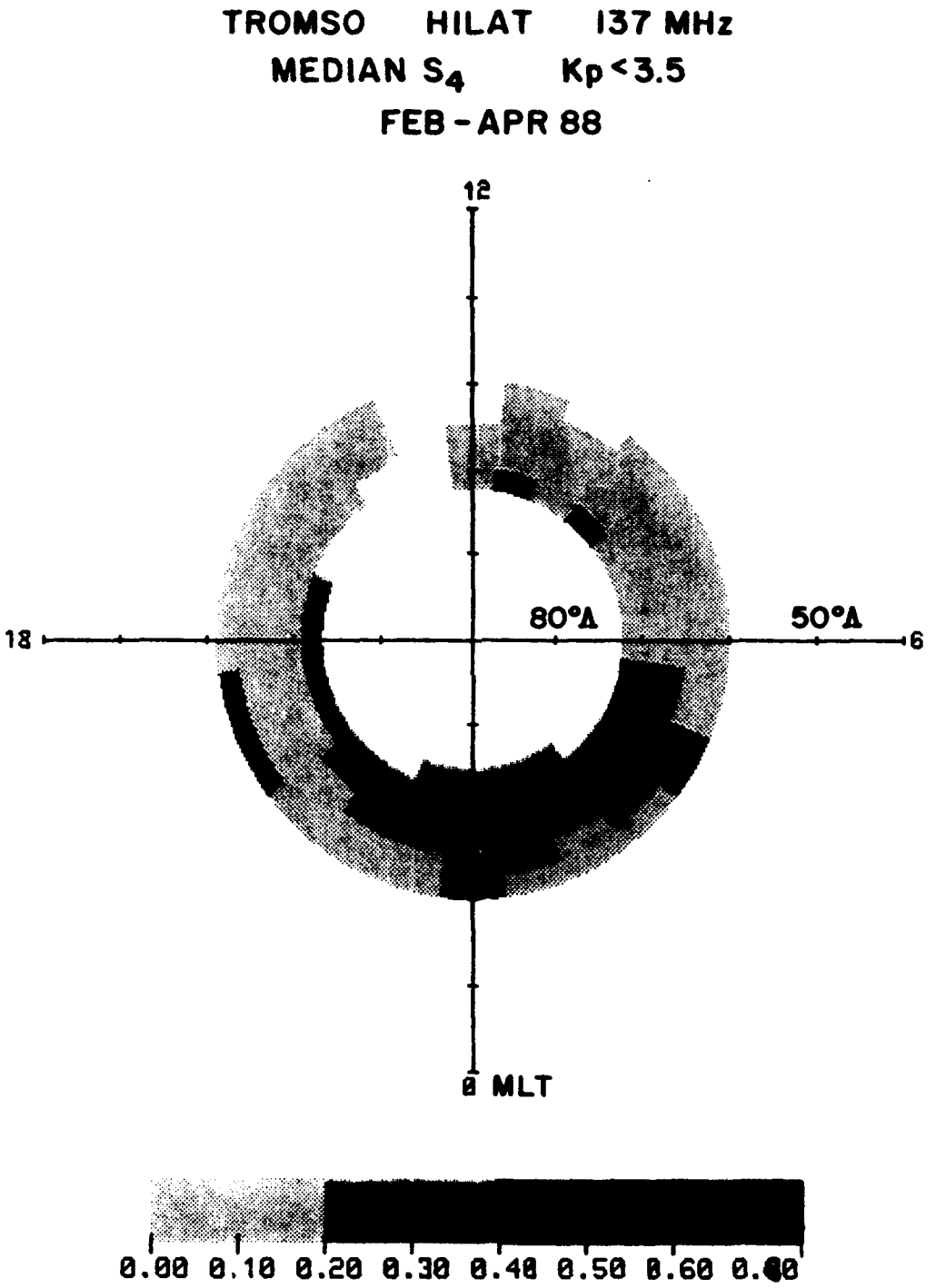
TROMSO HILAT 137 MHz
MEDIAN S_4 Kp<3.5
FEB-APR 88
12
18
6
80°Λ
50°Λ
0 MLT
0.00 0.10 0.20 0.30 0.40 0.50 0.60 0.80

Figure 4b.

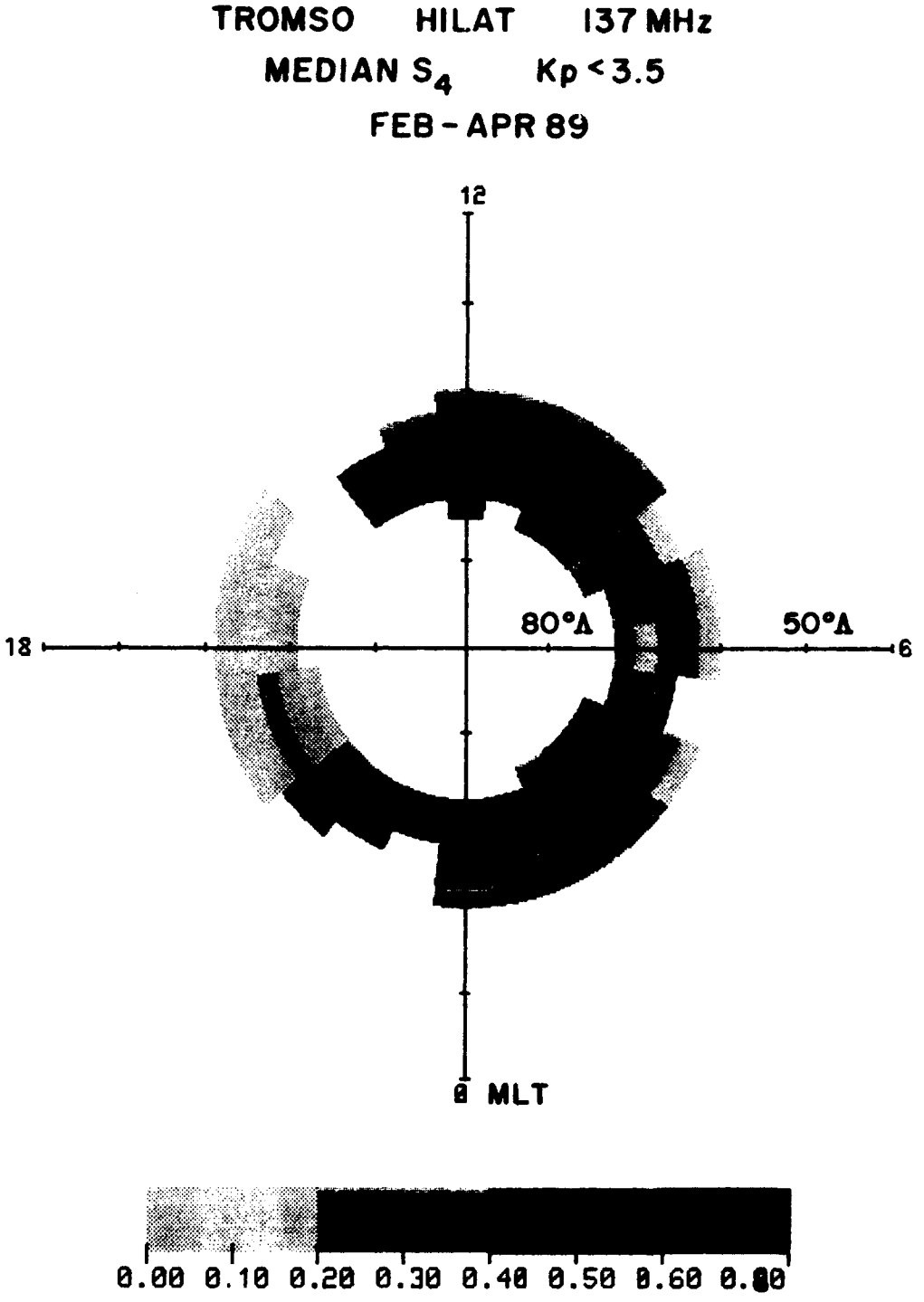
TROMSO HILAT 137 MHz
MEDIAN S_4 Kp < 3.5
FEB - APR 89
12
18
6
80°Λ
50°Λ
0 MLT
0.00 0.10 0.20 0.30 0.40 0.50 0.60 0.80

Figure 4c.

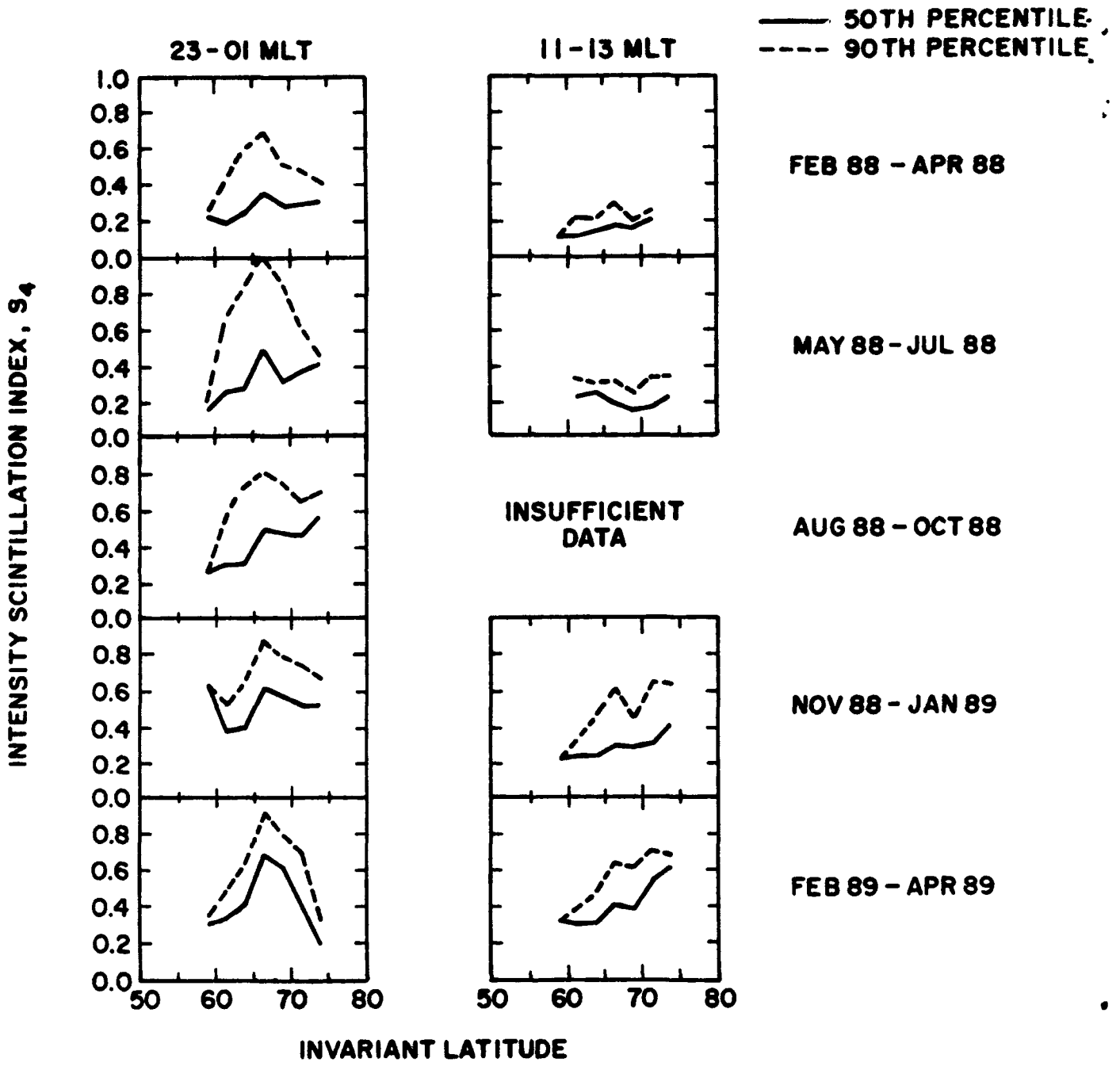
TROMSO HILAT S_4 137 MHz Kp < 3.5
50TH PERCENTILE
90TH PERCENTILE
23 - 01 MLT
11 - 13 MLT
FEB 88 - APR 88
MAY 88 - JUL 88
INSUFFICIENT DATA
AUG 88 - OCT 88
NOV 88 - JAN 89
FEB 89 - APR 89
INTENSITY SCINTILLATION INDEX, S_4
1.0
0.8
0.6
0.4
0.2
0.0
50
60
70
80
INVARIANT LATITUDE

Figure 5.

TROMSO HILAT

MEDIAN ION DENSITY Kp < 3.5

FEB - APR 84

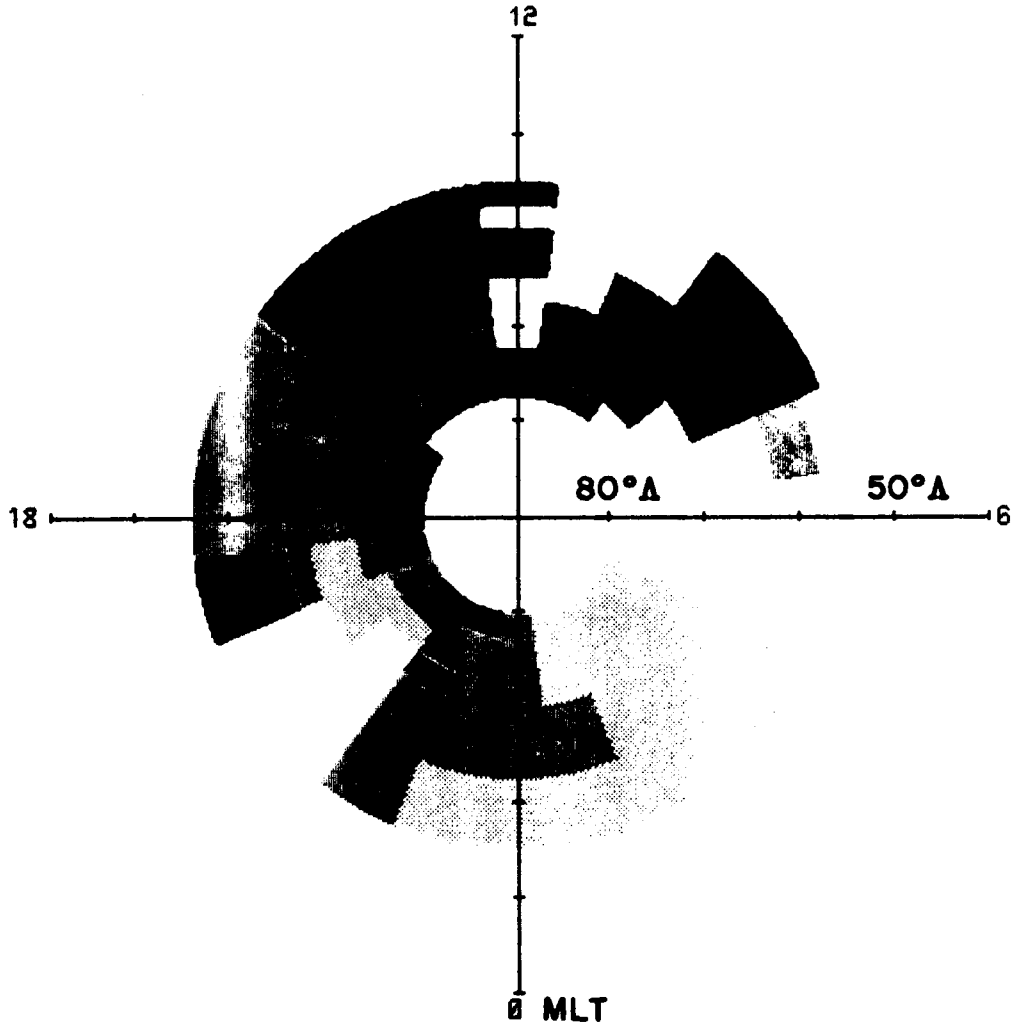

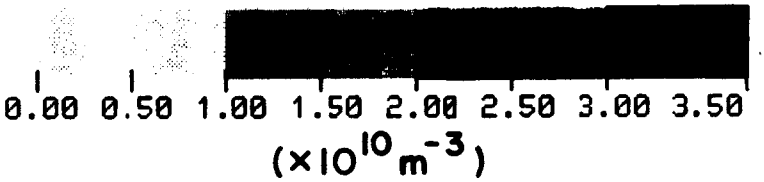

Figure 6a.

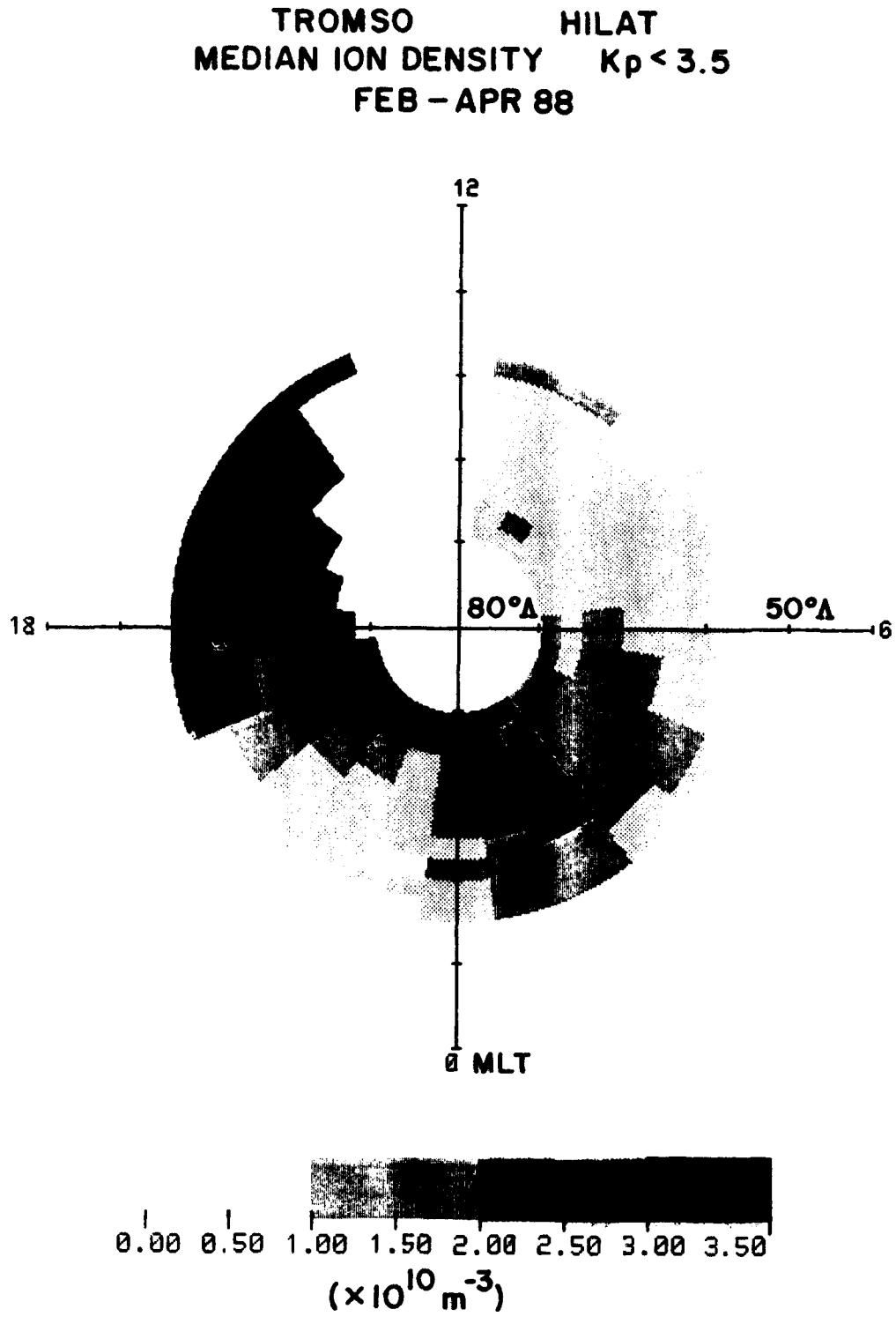
TROMSO HILAT
MEDIAN ION DENSITY Kp < 3.5
FEB – APR 88
12
18
80°Λ
50°Λ
6
0 MLT
0.00 0.50 1.00 1.50 2.00 2.50 3.00 3.50
(×10^10 m^-3)

Figure 6b.

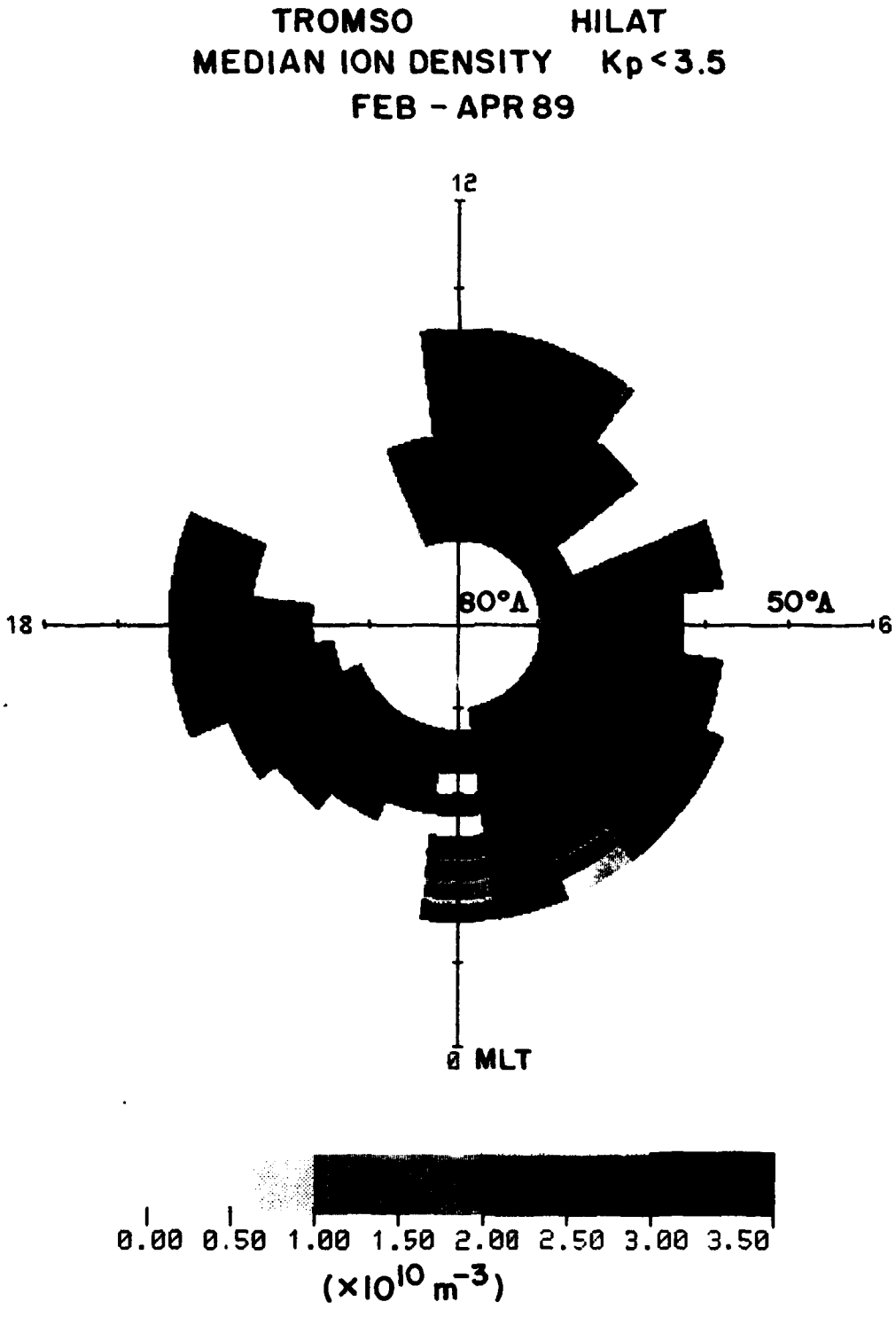
TROMSO HILAT
MEDIAN ION DENSITY Kp < 3.5
FEB - APR 89
12
18
80°Λ
50°Λ
6
0 MLT
0.00 0.50 1.00 1.50 2.00 2.50 3.00 3.50
(×10^10 m^-3)

Figure 6c.

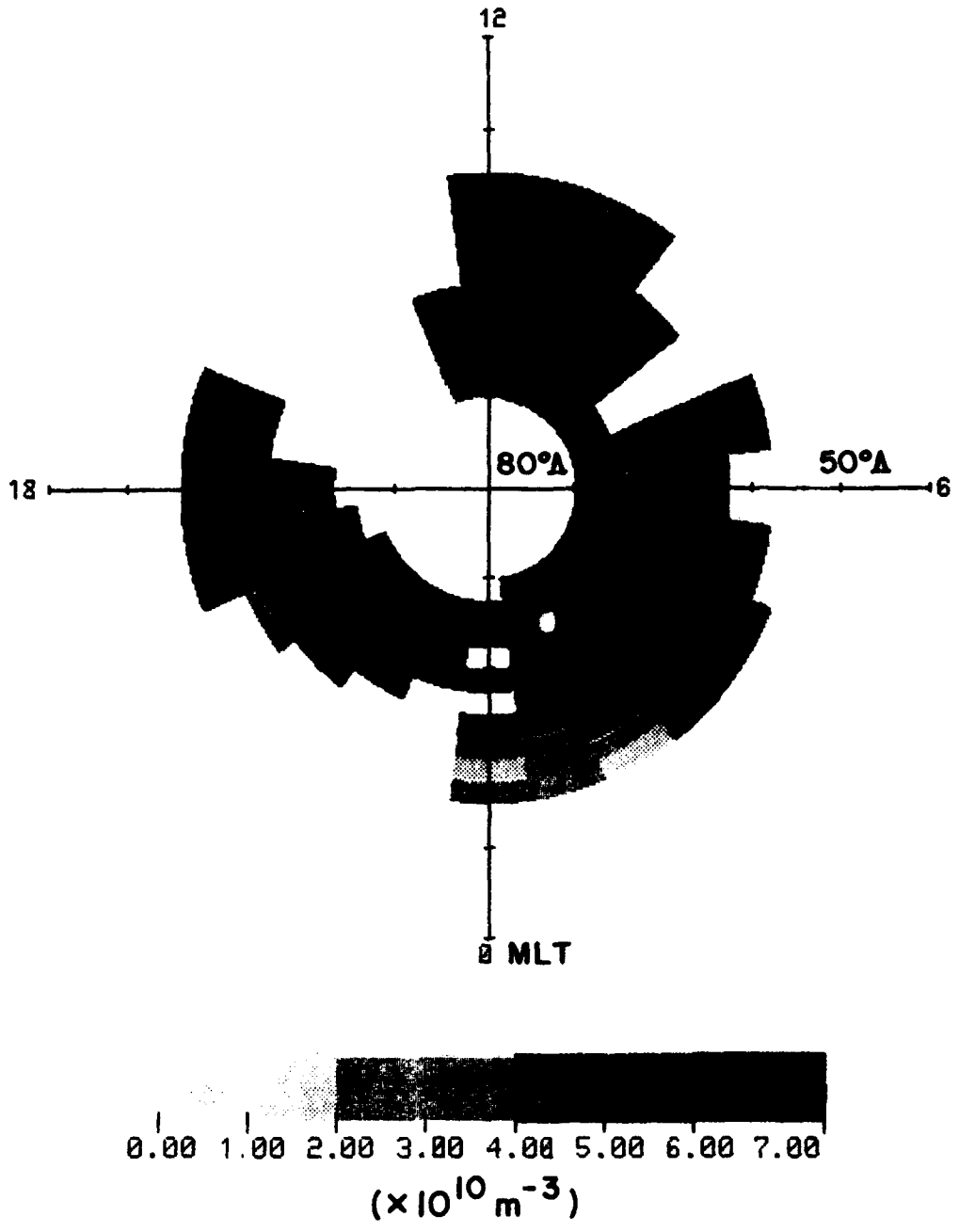
TROMSO HILAT
MEDIAN ION DENSITY Kp<3.5
FEB - APR 89
12
80°Λ
50°Λ
18
6
0 MLT
0.00 1.00 2.00 3.00 4.00 5.00 6.00 7.00
(×10^10 m^-3)

Figure 6d.

TROMSO HILAT ION DENSITY 137 MHz Kp < 3.5

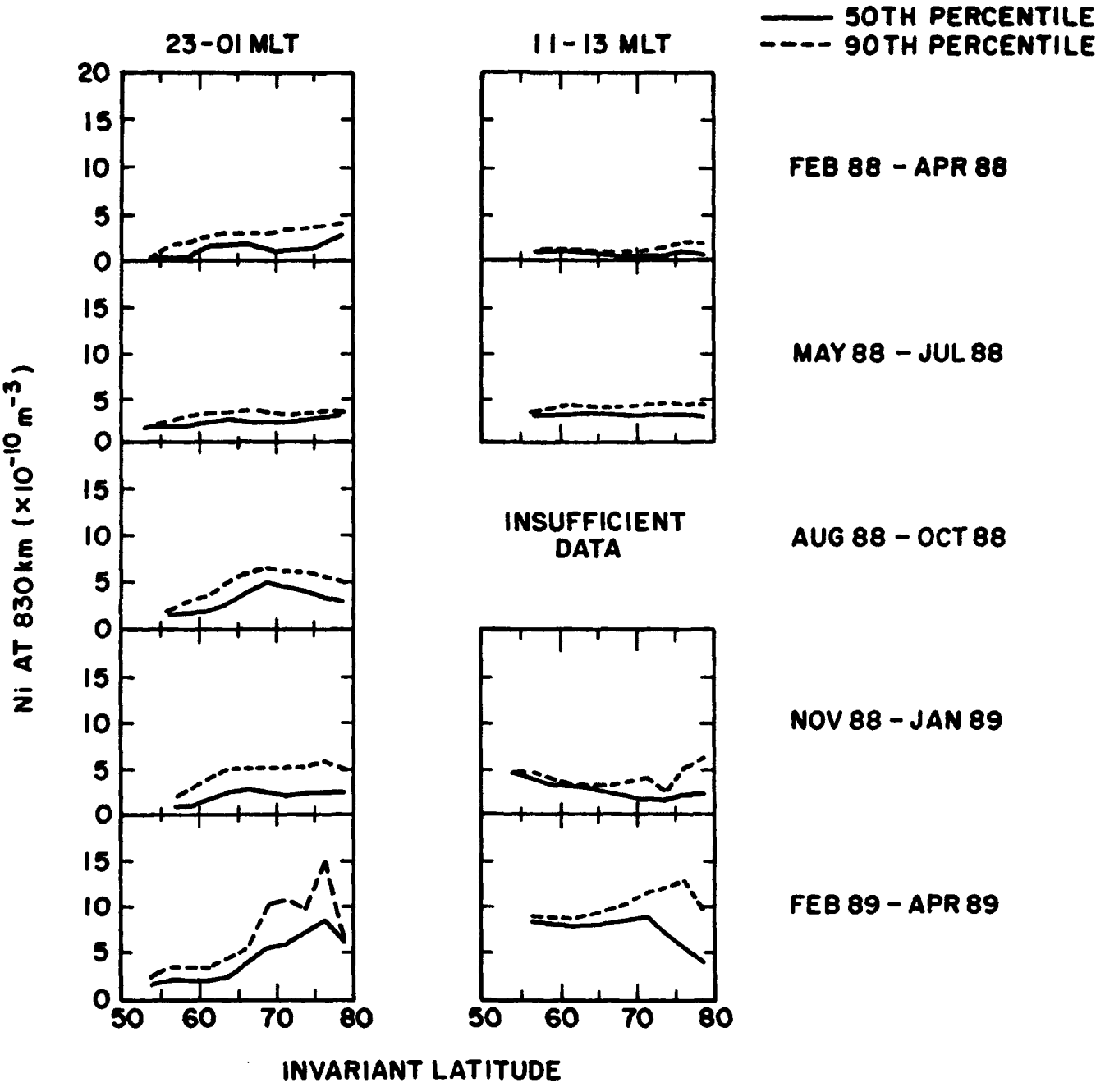

Figure 7.

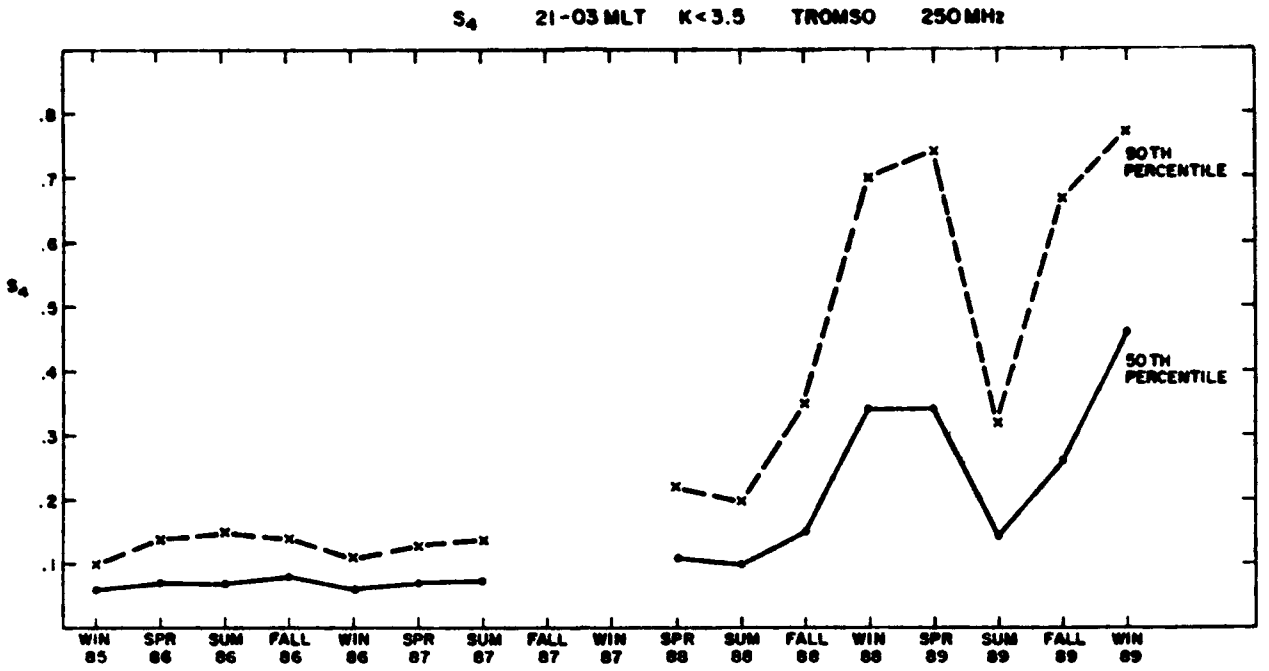
S_4 21-03 MLT K<3.5 TROMSO 250 MHz
S_4
.8
.7
.6
.5
.4
.3
.2
.1
90TH PERCENTILE
50TH PERCENTILE
WIN 85
SPR 86
SUM 86
FALL 86
WIN 86
SPR 87
SUM 87
FALL 87
WIN 87
SPR 88
SUM 88
FALL 88
WIN 88
SPR 89
SUM 89
FALL 89
WIN 89

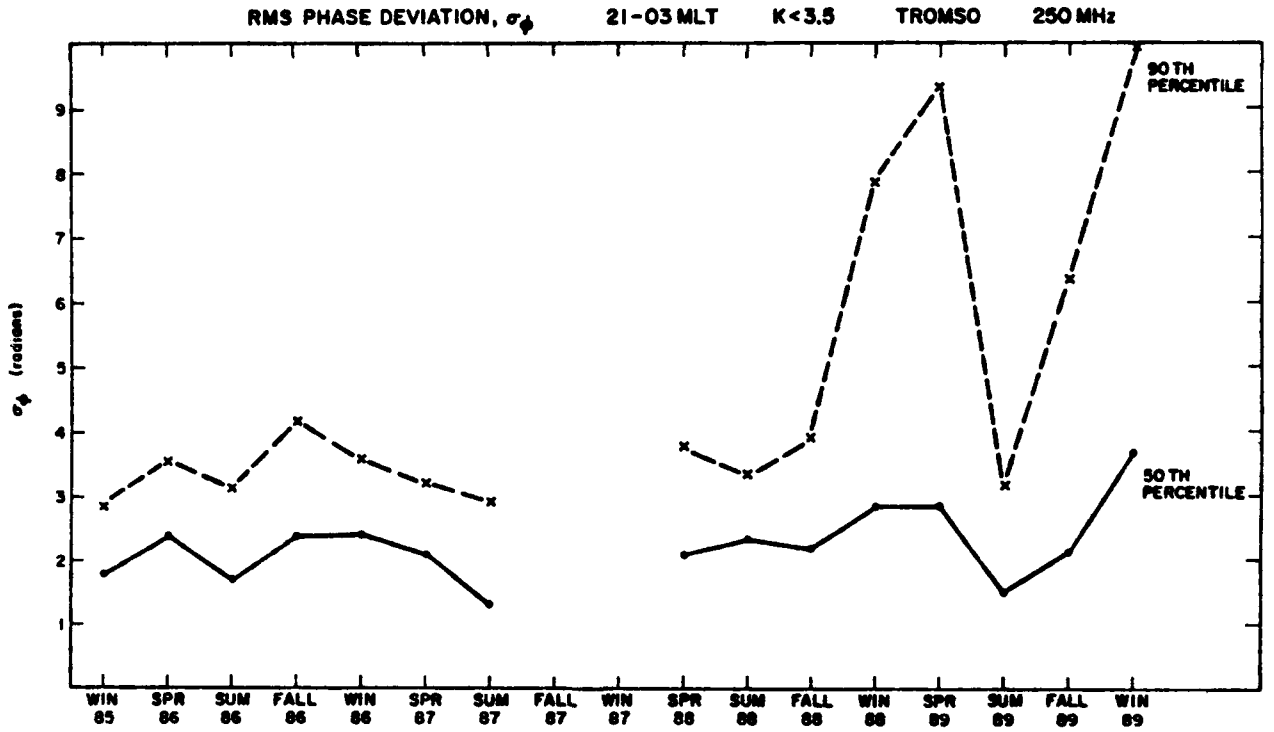
RMS PHASE DEVIATION, σ_ϕ 21-03 MLT K<3.5 TROMSO 250 MHz
σ_ϕ (radians)
9
8
7
6
5
4
3
2
1
90TH PERCENTILE
50TH PERCENTILE
WIN 85
SPR 86
SUM 86
FALL 86
WIN 86
SPR 87
SUM 87
FALL 87
WIN 87
SPR 88
SUM 88
FALL 88
WIN 88
SPR 89
SUM 89
FALL 89
WIN 89

Figure 8.

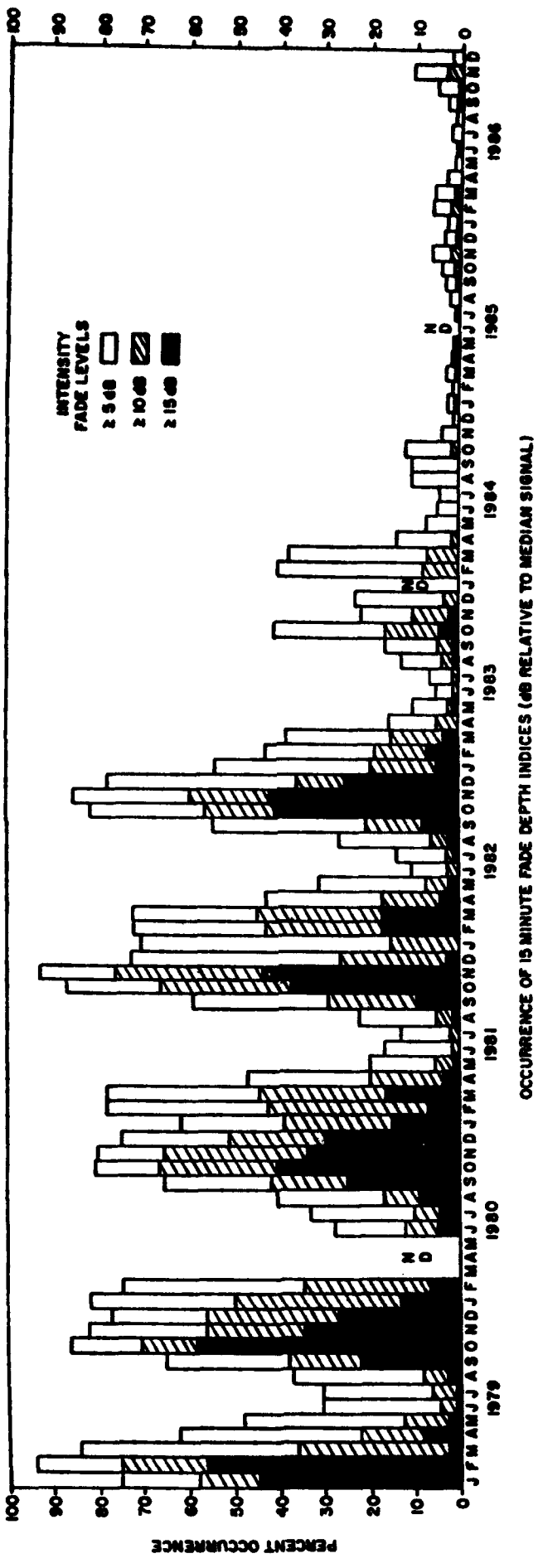
THULE K=0-9 250MHz
INTENSITY FADE LEVELS
≥ 5 dB
≥ 10 dB
≥ 15 dB
PERCENT OCCURRENCE
OCCURRENCE OF 15 MINUTE FADE DEPTH INDICES (dB RELATIVE TO MEDIAN SIGNAL)
1979
1980
1981
1982
1983
1984
1985
1986

Figure 9a.

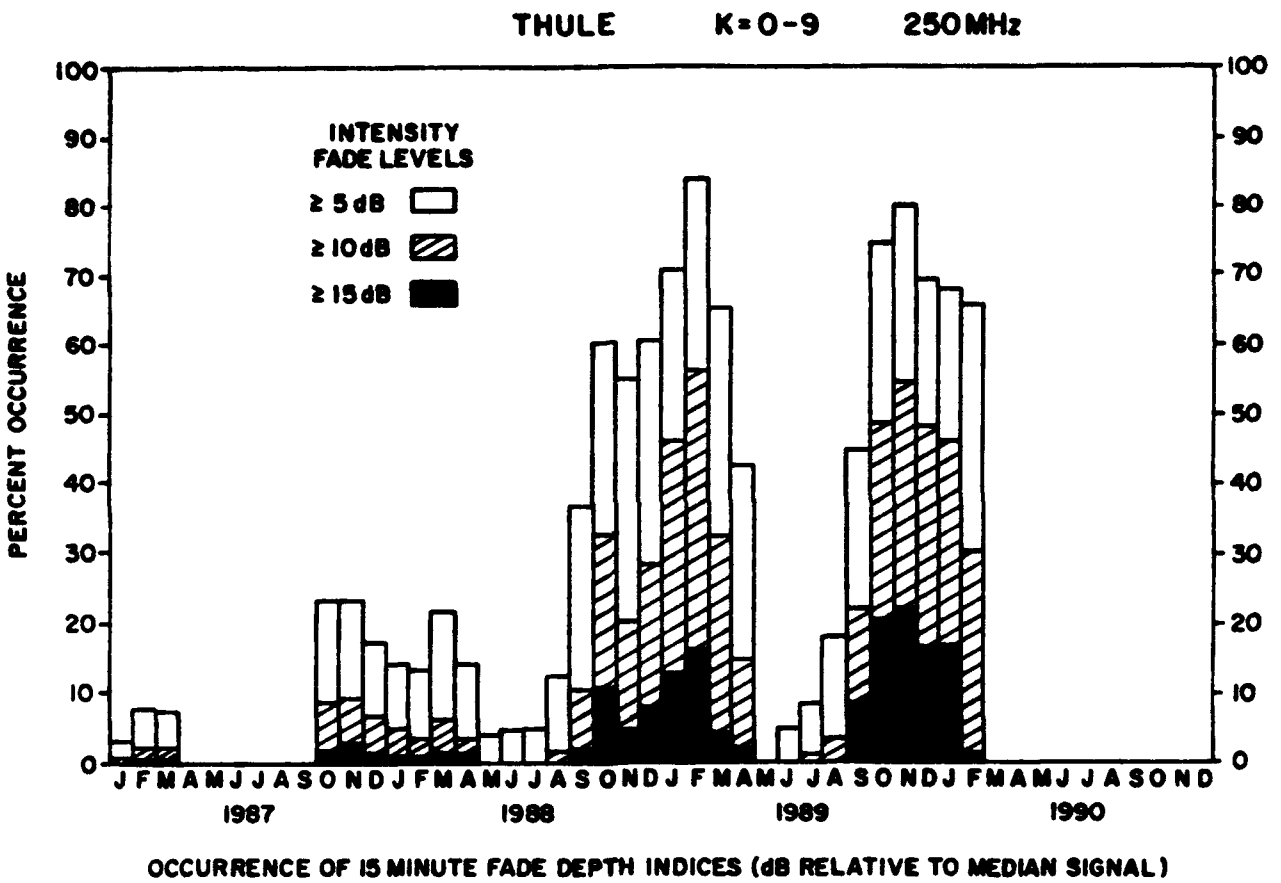
THULE K=0-9 250MHz
INTENSITY FADE LEVELS
≥ 5dB
≥ 10dB
≥ 15dB
PERCENT OCCURRENCE
0
10
20
30
40
50
60
70
80
90
100
J F M A M J J A S O N D J F M A M J J A S O N D J F M A M J J A S O N D J F M A M J J A S O N D
1987
1988
1989
1990
OCCURRENCE OF 15 MINUTE FADE DEPTH INDICES (dB RELATIVE TO MEDIAN SIGNAL)

Figure 9b.

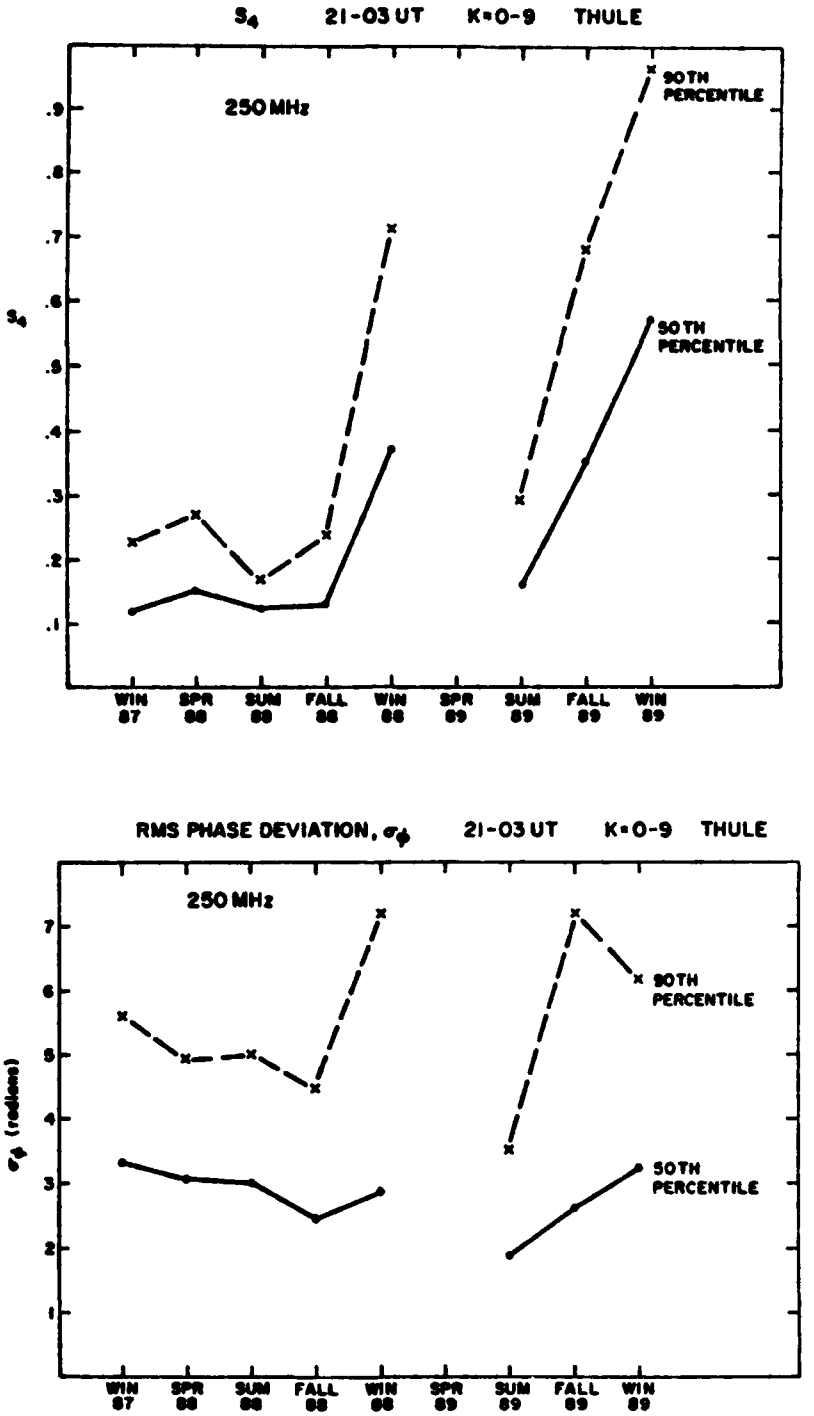
S_4 21-03 UT K=0-9 THULE
250 MHz
90TH PERCENTILE
50TH PERCENTILE
S_4
.9
.8
.7
.6
.5
.4
.3
.2
.1
WIN 87
SPR 88
SUM 88
FALL 88
WIN 88
SPR 89
SUM 89
FALL 89
WIN 89
RMS PHASE DEVIATION, σ_ϕ 21-03 UT K=0-9 THULE
250 MHz
90TH PERCENTILE
50TH PERCENTILE
σ_ϕ (radians)
7
6
5
4
3
2
1
WIN 87
SPR 88
SUM 88
FALL 88
WIN 88
SPR 89
SUM 89
FALL 89
WIN 89

Figure 10.

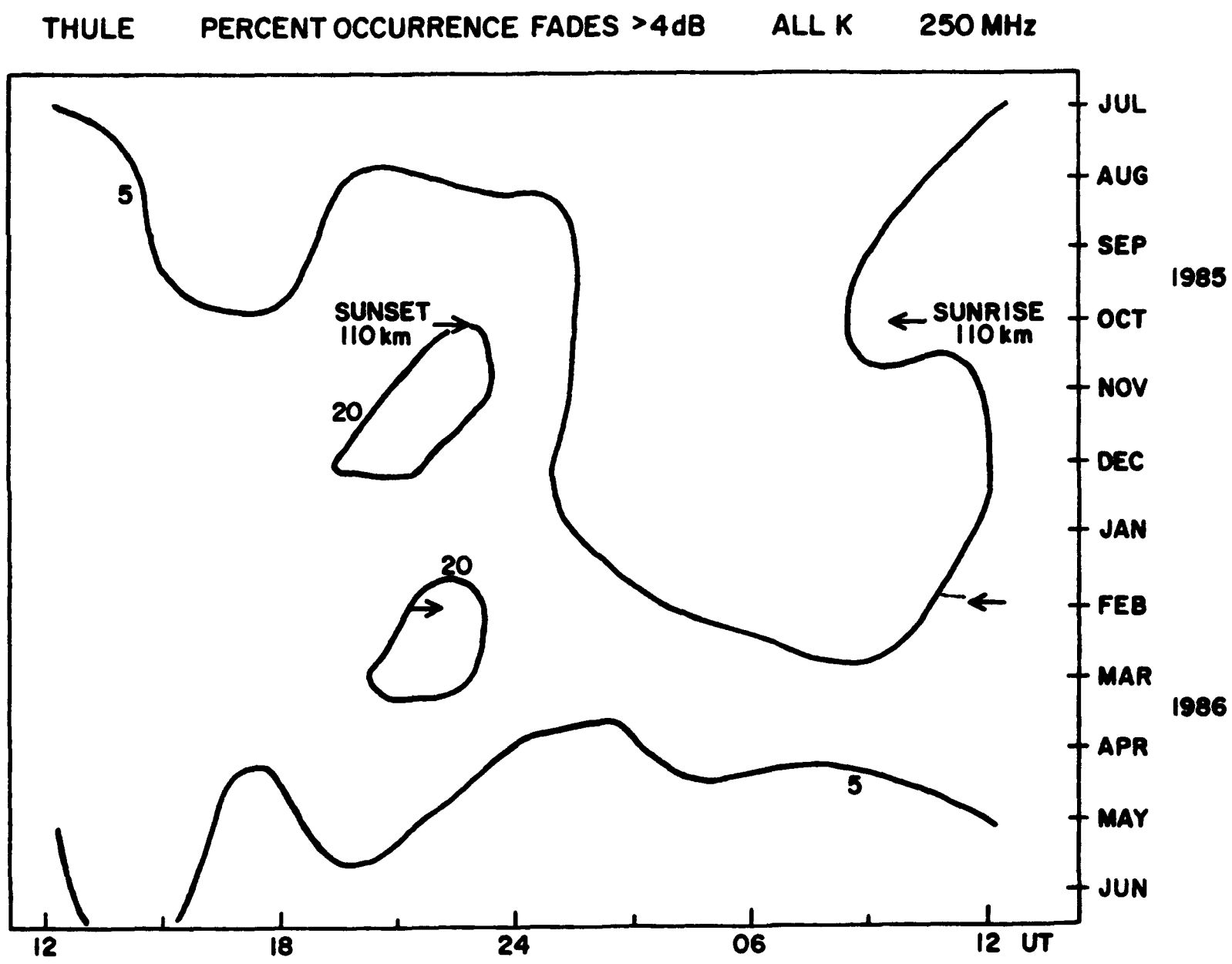
THULE PERCENT OCCURRENCE FADES >4dB ALL K 250 MHz
5
SUNSET
110 km
20
20
SUNRISE
110 km
5
JUL
AUG
SEP
1985
OCT
NOV
DEC
JAN
FEB
MAR
1986
APR
MAY
JUN
12
18
24
06
12 UT

Figure 11.

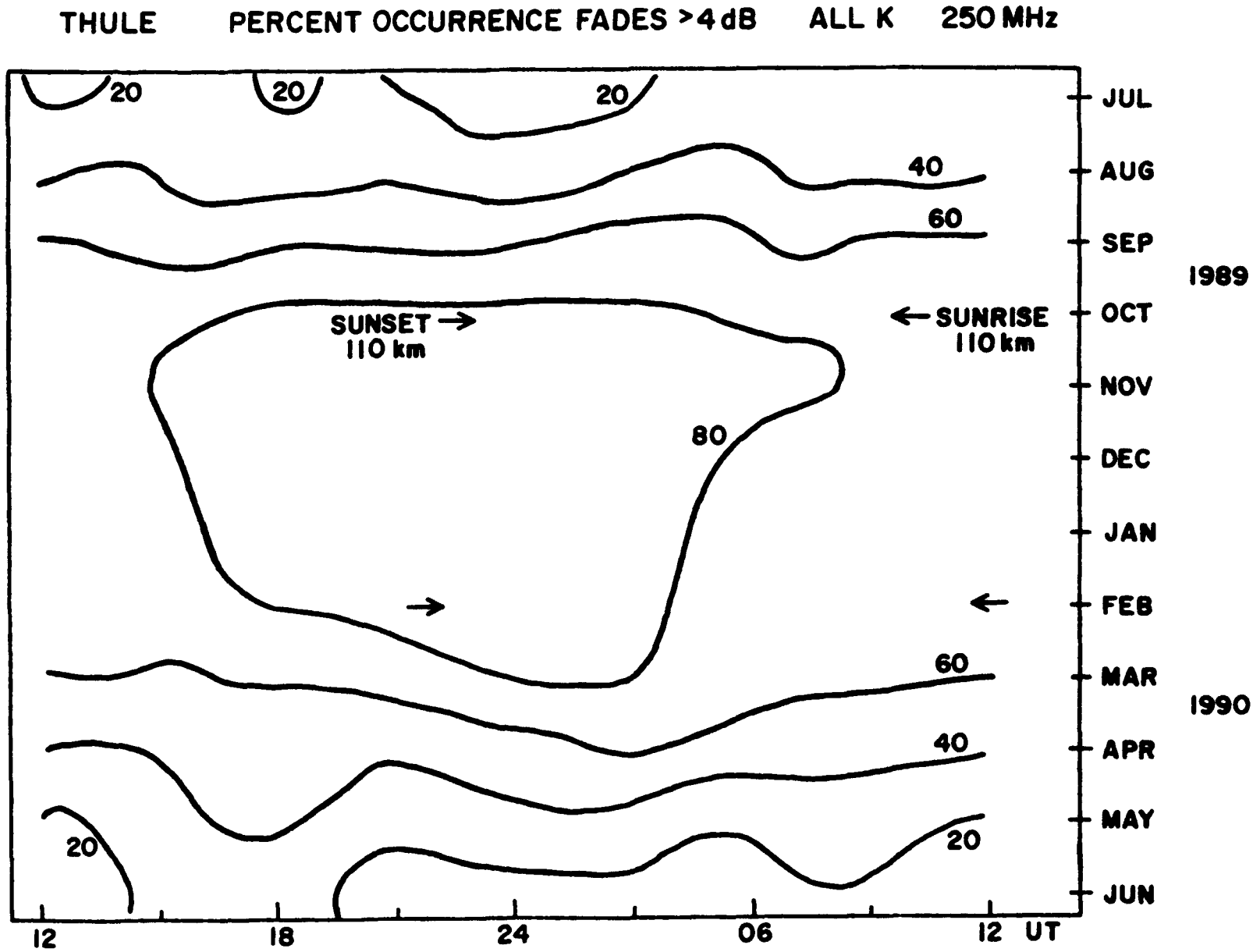
THULE PERCENT OCCURRENCE FADES >4 dB ALL K 250 MHz
20
20
20
40
60
SUNSET →
110 km
← SUNRISE
110 km
80
60
40
20
20
JUL
AUG
SEP
OCT
NOV
DEC
JAN
FEB
MAR
APR
MAY
JUN
1989
1990
12
18
24
06
12 UT

Figure 12.

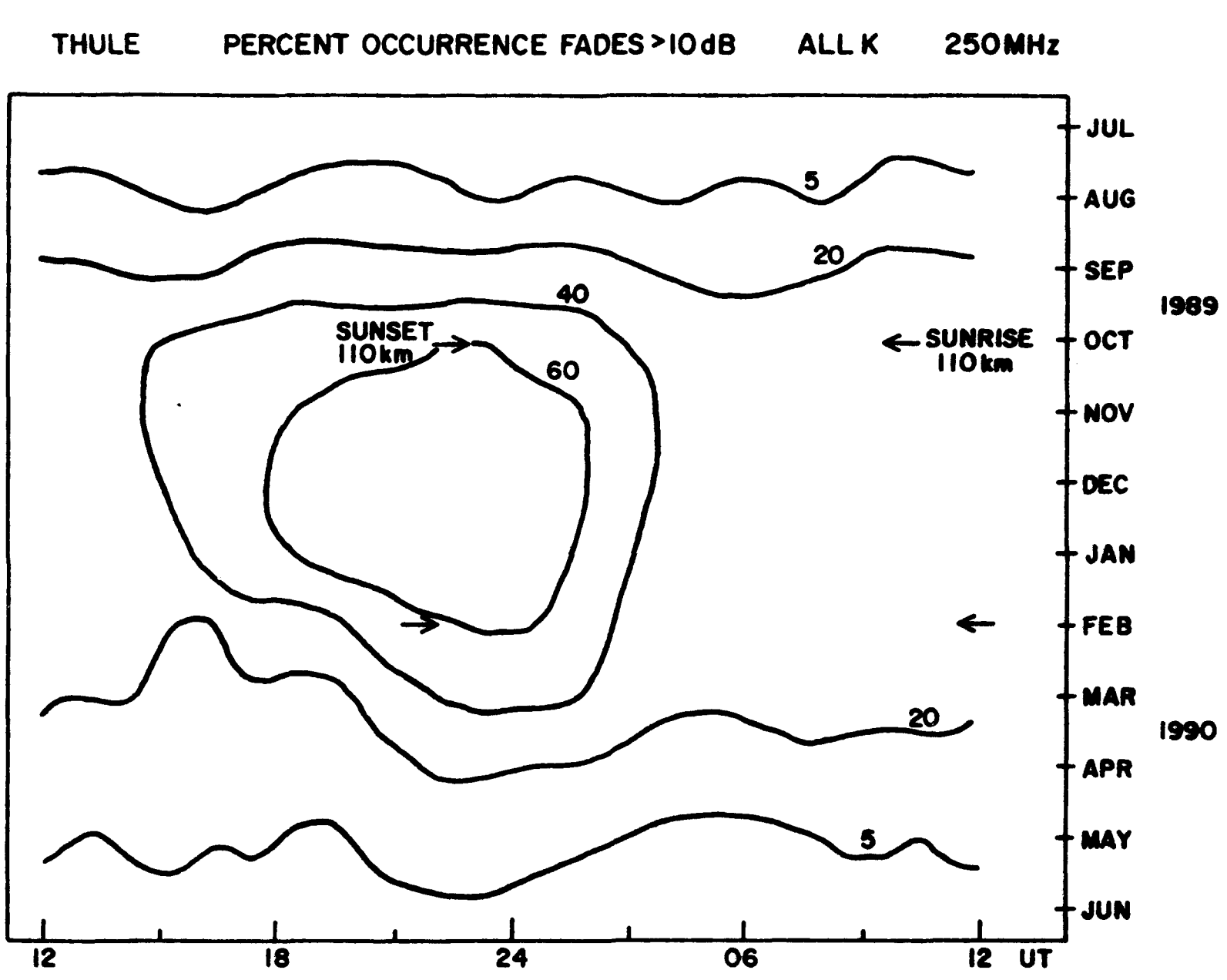
THULE PERCENT OCCURRENCE FADES >10dB ALL K 250MHz
JUL
AUG
SEP
OCT
NOV
DEC
JAN
FEB
MAR
APR
MAY
JUN
1989
1990
5
20
40
60
20
5
SUNSET
110km
SUNRISE
110km
12
18
24
06
12
UT

Figure 13.